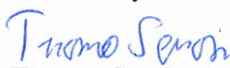

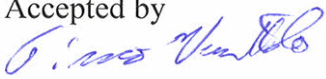


# MELCOR Modeling of a Passive Containment Cooling System Experiment PANDA T1.1

Author: Tuomo Sevón

Confidentiality: Public

Report's title	
MELCOR Modeling of a Passive Containment Cooling System Experiment PANDA T1.1	
Customer, contact person, address	Order reference
SAFIR2014 research program	25/2011SAF
Project name	Project number / Short name
Thermal Hydraulics of Severe Accidents	73498 / TERMOSAN2011
Author	Pages
Tuomo Sevón	54
Keywords	Report identification code
Nuclear safety, passive containment cooling system, condenser, PCCS, PANDA, MELCOR	VTT-R-01433-12
<p>Summary</p> <p>Modeling passive containment cooling systems with the MELCOR code was investigated. First, a literature review of passive containment condenser experiments was performed, and the published experiments are summarized in this report. Two experiments were selected for MELCOR 2.1 calculations.</p> <p>Simple experiments on condensation and aerosol deposition in a vertical tube were used for validation calculations of MELCOR's condensation and deposition models. The calculated condensation rates were within 8 % of the measurements. The calculated aerosol deposition was within 10 percentage units from the measurements.</p> <p>PANDA T1.1 experiment, which investigated the ESBWR containment behavior in a severe accident, was calculated with MELCOR. It was found out that careful modeling of drainage of the condensed water is important. With default treatment, the water formed tiny levitating pools inside the condenser. This caused numerical difficulties and serious oscillation to the results. Guiding the condensed water directly out of the condenser eliminated this problem. There was some uncertainty in the amount of helium injected to the PANDA facility. The calculations were made with 75 kg of helium. This amount was inferred from mass spectrometer measurements. According to the test report, 92 kg of helium was injected, but this appears to be an overestimation.</p> <p>It is concluded that MELCOR was able to calculate the condenser performance in the PANDA experiment with 7 % accuracy. This is sufficient for using the model in full plant calculations.</p>	
Confidentiality	Public
Espoo 22.2.2012	
Written by	Reviewed by
	
Tuomo Sevón Senior Scientist	Ismo Karppinen Senior Scientist
	Accepted by
	
	Timo Vanttola Technology Manager
VTT's contact address	
VTT, P.O.Box 1000, FI-02044 VTT, Finland	
<p>Distribution (customer and VTT)</p> <p>Risto Sairanen, Lauri Pöllänen, Tomi Routamo /STUK; Antti Tarkiainen, Janne Vahero /TVO; Marko Marjamäki, Mika Harti /Fortum; Nici Bergroth /Fennovoima; Jarmo Ala-Heikkilä /Aalto; Heikki Suikkanen, Heikki Purhonen /LUT; Iona Lindholm, Arja Saarenheimo, Ismo Karppinen, Ari Auvinen, Timo Vanttola, Kaisa Simola, Vesa Suolanen, Seppo Hillberg, Niina Könönen, Anna Nieminen, Jan-Erik Holmberg, Ilkka Männistö /VTT; Domenico Paladino /PSI</p>	
<p><i>The use of the name of the VTT Technical Research Centre of Finland (VTT) in advertising or publication in part of this report is only permissible with written authorisation from the VTT Technical Research Centre of Finland.</i></p>	

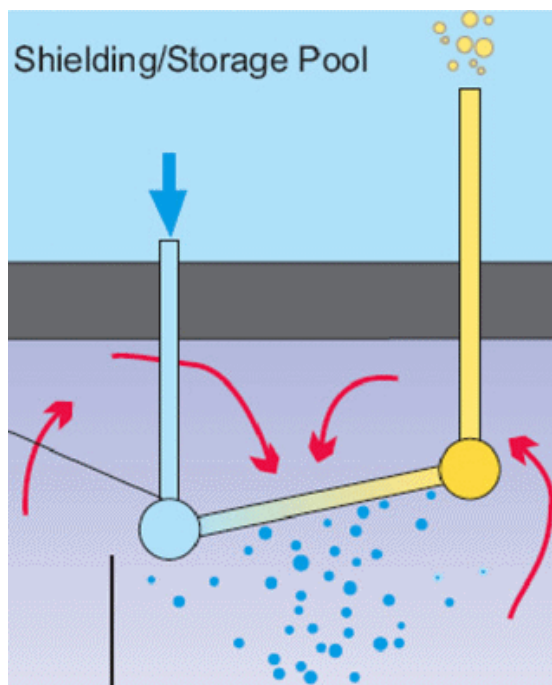
## Contents

1	Introduction.....	4
2	A Literature Review of PCCS Experiments.....	5
2.1	Passive Containment Condenser Experiments.....	5
2.1.1	GIRAFFE Experiments.....	5
2.1.2	INKA Experiments.....	6
2.1.3	Maheshwari et al. Experiments.....	7
2.1.4	NOKO Experiments.....	8
2.1.5	PANDA Experiments.....	8
2.1.6	PANTHERS Experiments.....	12
2.1.7	PUMA Experiments.....	13
2.1.8	ROSA/LSTF Experiments.....	14
2.1.9	TIGER Experiments.....	15
2.1.10	Summary of Passive Containment Condenser Experiments.....	15
2.2	Experiments on Aerosol Deposition in Condensers.....	15
2.2.1	AIDA Experiment.....	16
2.2.2	CESANE and STORM Experiments.....	16
2.2.3	Gröhn et al. Experiments.....	17
2.2.4	Lehtinen et al. Experiments.....	18
2.2.5	Suonmaa Experiments.....	18
2.2.6	Summary of Experiments on Aerosol Deposition in Condensers.....	19
3	MELCOR Modeling of Lehtinen et al. Condensation and Aerosol Deposition Experiments.....	19
3.1	Model.....	20
3.2	Results.....	21
4	MELCOR Modeling of PANDA T1.1 Experiment.....	22
4.1	Modeling the Vessels and Pipelines.....	22
4.1.1	RPV Vessel.....	22
4.1.2	Drywells.....	24
4.1.3	Wetwells.....	25
4.1.4	GDCS Tank.....	27
4.1.5	Flow Resistance of Pipelines.....	28
4.1.6	Heat Losses from the Facility.....	28
4.1.7	Gas Consumption of the Mass Spectrometer.....	28
4.1.8	Helium Injection.....	29
4.2	Modeling the PCC Units.....	31
4.2.1	Nodalization.....	31
4.2.2	Heat Loss from the Pool.....	33
4.2.3	Condensate Drainage Modeling.....	33
4.3	Results.....	34
4.3.1	Base Case.....	34

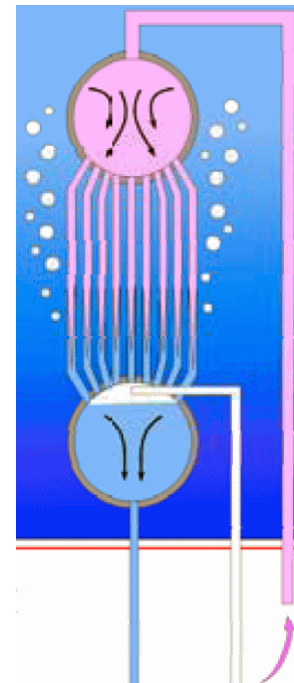
4.3.1.1	Pressures and Flow Rates .....	34
4.3.1.2	Temperatures .....	39
4.3.1.3	Helium Concentrations .....	44
4.3.2	Simplified PCC Nodalization .....	46
4.3.3	Increased Heating Power .....	47
5	Conclusions .....	48
	References .....	51

## 1 Introduction

Many new nuclear reactor concepts utilize passive condensers for removing heat from the containment atmosphere in the case of an accident. Reactor types that have been considered for construction in Finland have two basic condenser types. In the first, water circulates in inclined tubes that are placed in the containment atmosphere, and steam condenses on the outer surfaces of the tubes (Fig. 1). This concept is used in Areva's Kerena reactor design, former SWR-1000 (Stosic et al. 2008), and in Atomstroyexport's AES-2006 design (STUK 2009). In the second condenser type, steam from the containment flows in tubes that are immersed in a water pool (Fig. 2). In this case the steam condenses inside the tubes. This concept is used in GE Hitachi's ESBWR (Beard 2006). A version of Toshiba-Westinghouse's ABWR design would have a condenser of the second type, where steam condenses inside the tubes, but the tubes are horizontal (Arai et al. 2008).



**Fig. 1.** Passive condenser in Kerena reactor concept, steam condensing outside the tube (Stosic et al. 2008).



**Fig. 2.** Passive condenser in ESBWR, steam condensing inside the tube (Beard 2006).

The work on MELCOR modeling of passive containment cooling systems (PCCS) was started earlier by simulating experiments on steam condensation in a tube in the presence of air (Sevón 2010). These Purdue University experiments were not passive condenser tests because the steam and air were actively injected into the tube. It was found out that, with the default parameters, MELCOR underestimates the condensation rate by about 20 %, both with pure steam and with steam–air mixtures. The reason for the underestimation was found in the Reynolds number limits that MELCOR uses to classify the condensate film flow as laminar or turbulent. MELCOR's default film Reynolds number limits are 1000 and 3000, while Incropera & DeWitt (2002) recommend 30 and 1800. The film Reynolds number limits are coded as sensitivity coefficients 4253(5) and 4253(6). Changing these to the lower values improved the MELCOR results significantly. The MELCOR model with the modified Reynolds number limits simulates the experiments with an average deviation of 3.5 %, which is close to the measurement uncertainties.

Chapter 2 of this report presents a literature review of passive containment cooling system experiments and of experiments on aerosol deposition in condensers. Chapter 3 extends the Sevón (2010) MELCOR validation calculations to higher non-condensable gas concentrations. Also the aerosol deposition in the condenser tubes is compared with MELCOR results. Chapter 4 presents a MELCOR simulation of the integral PANDA T1.1 experiment related to ESBWR-type passive containment condensers.

## 2 A Literature Review of PCCS Experiments

This chapter documents a literature review of passive containment cooling system (PCCS) experiments. The text is divided into two parts. Section 2.1 concerns passive containment condenser experiments. Section 2.2 deals with experiments on aerosol deposition in condensers.

### 2.1 Passive Containment Condenser Experiments

This literature review includes only experiments that were truly passive or that employed a complete containment condenser unit. Condensation experiments where the steam was actively injected into a simple tube are excluded. A list of this kind of experiments is available in (Zhou et al. 2010). Also excluded are experiments on passive core cooling systems, even though they can have similar geometries as containment cooling systems.

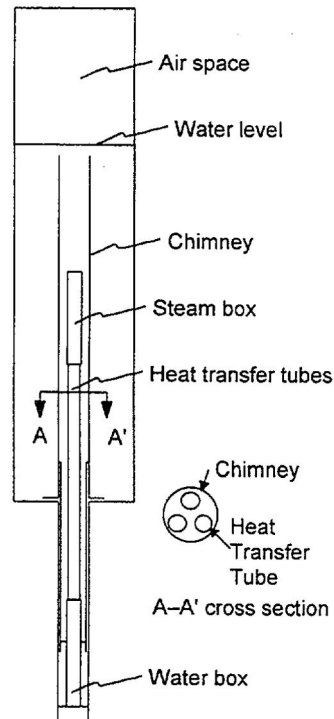
#### 2.1.1 GIRAFFE Experiments

GIRAFFE (Gravity-Driven Integral Full-Height Test Facility for Passive Heat Removal) experiments have been performed by Toshiba in Japan. An overview of the test series is presented in (Kataoka et al. 1998). Construction of the facility was started in 1989. It simulated the containment of the SBWR (Simplified Boiling Water Reactor), which was a forerunner of the ESBWR (Economic Simplified Boiling Water Reactor).

GIRAFFE has a 1:1 height scale to the SBWR design; the total height of the facility is 30 m. The volumetric scale is 1:400. The facility consists of five vessels:

1. PCCS pool, providing cooling water to the secondary side of the condenser
2. Drywell
3. Reactor pressure vessel (RPV), containing an electric heater to generate steam, which is discharged to the drywell.
4. Suppression chamber, containing the suppression pool. It is connected to the drywell with two pipes, simulating the vent line (under water) and the vacuum breaker (above the suppression pool water level). If the drywell pressure is sufficiently much above the suppression chamber pressure, the vent line opens. If the suppression chamber pressure is higher than the drywell pressure, the vacuum breaker opens.
5. GDSC (Gravity-Driven Cooling System) pool. It is connected to the drywell by a pressure equalizing line and to the RPV by a drain line.

The PCCS heat exchanger is shown in Fig. 3. A pipeline (not in the figure) from the drywell brings steam and non-condensable gases to the steam box. The water box is connected to the GDSC with the drain line and to the suppression pool with the vent line. Between the steam box and the water box there are three vertical heat transfer tubes with inner diameter of 46 mm and length of 1.8 m. In the PCCS pool, a chimney separates the boiling region from the subcooled region.



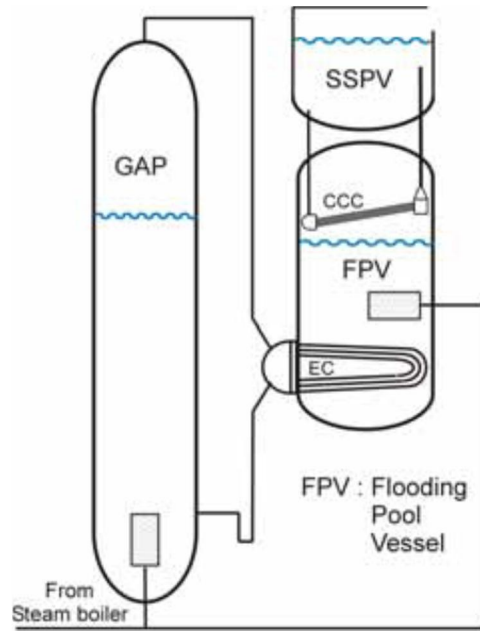
**Fig. 3.** PCCS heat exchanger in the GIRAFFE facility (Kataoka et al. 1998).

Toshiba has performed both separate effect and system integral tests in the GIRAFFE facility. In the separate effect tests, steam along with nitrogen or helium was injected to the steam box under forced flow conditions, in order to investigate the heat transfer degradation due to the non-condensable gases. Nitrogen causes a slightly larger reduction in heat transfer than the same volume fraction of helium due to nitrogen's lower thermal conductivity. Helium is quite a good simulant of hydrogen. In the system integral tests, the facility was used in the passive mode with various initial and boundary conditions, simulating different accident scenarios. The GIRAFFE results have been used in the development and validation of the TRAC computer code, and some comparisons between the experiments and the calculations are provided in (Kataoka et al. 1998).

### 2.1.2 INKA Experiments

INKA (Integral-Versuchstand Karlstein) test facility is operated by Areva NP in Karlstein, Germany. It was constructed in 2008 for testing the passive safety systems of the Kerena reactor. The containment volume is scaled by 1:24, but the tested components are full scale, and the heights that are important for the operation of the passive components are the same as in the plant.

Areva has performed single component tests with the containment cooling condenser (Fig. 4). Steam was injected to the flooding pool vessel, and it was cooled passively by the condenser. Also the emergency condenser, for cooling the reactor core, has been tested in the same facility by injecting steam to the pressure vessel (GAP in the figure). Next Areva is proceeding with integral system tests, where the interplay of the passive components is tested. For the integral tests, the facility is complemented with two additional vessels, simulating the drywell and the suppression pool. (Leyer et al. 2010)



**Fig. 4.** INKA test facility configuration for single component tests. CCC means containment cooling condenser, EC is emergency condenser, and SSPV is shielding/storage pool vessel. (Leyer et al. 2008)

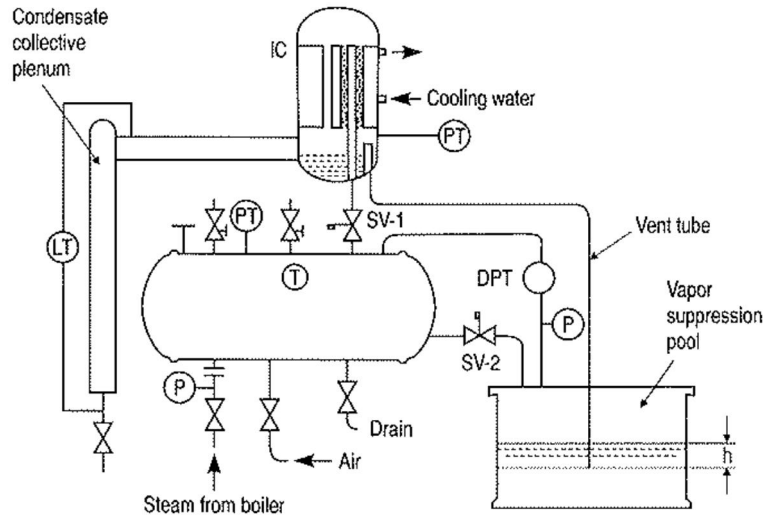
### 2.1.3 Maheshwari et al. Experiments

A passive containment cooling system that works with the same principle as the ESBWR system (Fig. 2) has been considered as one option for the Indian Advanced Heavy Water Reactor (AHWR). Bhabha Atomic Research Centre has performed experiments on such a device (Maheshwari et al. 2001). Since that time, the containment cooling system of the AHWR design has been changed to one that works with the same principle as the Kerena condenser (Fig. 1) (Sinha & Kakodkar 2006).

The Maheshwari et al. (2001) experimental set-up is shown in Fig. 5. Steam and air were injected to a vessel that simulates the drywell. From there the gases flowed through an insulated tube to the upper header of the condenser. During down-flow in the condenser, steam condensed in a tube or tubes. Cooling water was pumped to the secondary side. The condensed water was collected to the “collective plenum”, and gases were vented to the suppression pool through a submerged tube. The drywell vessel and the suppression pool vessel were connected by a vacuum breaker valve SV-2, which was opened when the suppression pool pressure exceeded the drywell pressure by a specified amount and reclosed after the pressures had equalized.

Experiments were performed with both constant and decreasing steam flow rates. The latter simulates the decreasing decay heat level. In the constant flow rate experiments, the drywell pressure remained above the suppression pool pressure, and thus the vacuum breaker valve did not open. Decreasing the steam flow rate caused the drywell pressure to drop below the suppression pool pressure, thus causing the vacuum breaker valve to open.



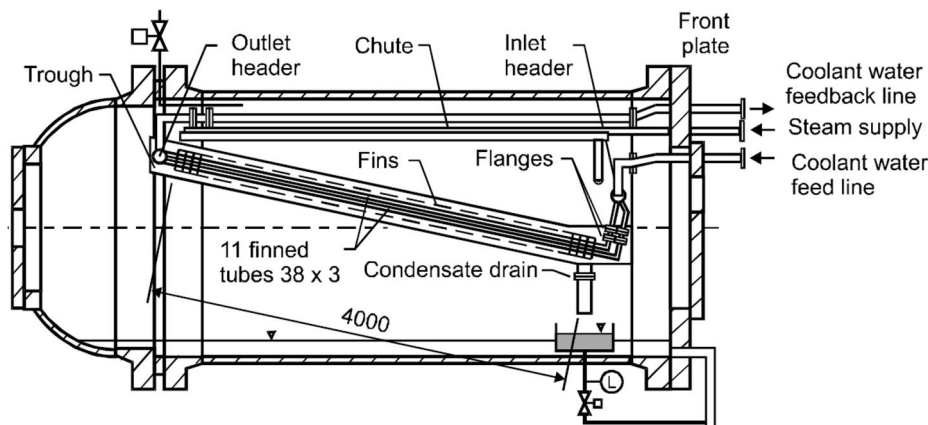


**Fig. 5.** Experimental set-up of Maheshwari et al. (2001).

#### 2.1.4 NOKO Experiments

NOKO (Notkondensator) experiments were performed at Forschungszentrum Jülich in Germany for investigating SWR-1000 passive safety systems. Both an emergency condenser (for core cooling) and a containment cooling condenser (which is called *building condenser* in NOKO publications) were tested. The facility operated from 1994 to 2000, after which it was moved to Forschungszentrum Rossendorf and renamed as TOPFLOW (Hicken et al. 2000). Publications of containment condenser tests at the TOPFLOW facility were not found.

The NOKO tank with a building condenser is shown in Fig. 6. Steam and non-condensable gases were injected to the tank, simulating the containment atmosphere. Coolant water was pumped into the finned tubes. So, the coolant water flow was not passive. This allowed reaching a steady state. Dozens of experiments have been performed at various pressures, flow rates and non-condensable gas concentrations. (Fethke et al. 1998)



**Fig. 6.** NOKO tank with a building condenser (Hicken et al. 2000).

#### 2.1.5 PANDA Experiments

PANDA (Passive Nachwärmeabfuhr und Druckabbau Testanlage) is operated by PSI in Switzerland. It has been used for testing passive containment condensers of the SBWR, ESBWR and SWR-1000 (Kerena) reactor designs. The SBWR (or ESBWR) PCC unit in the PANDA facility is shown in Fig. 7. It consists of a cylindrical upper header, 20 vertical tubes

and a cylindrical lower header. The inlet pipe is connected to the top of the upper header. The lower header has two connections: the vent pipe at the side and the drain pipe at the bottom.

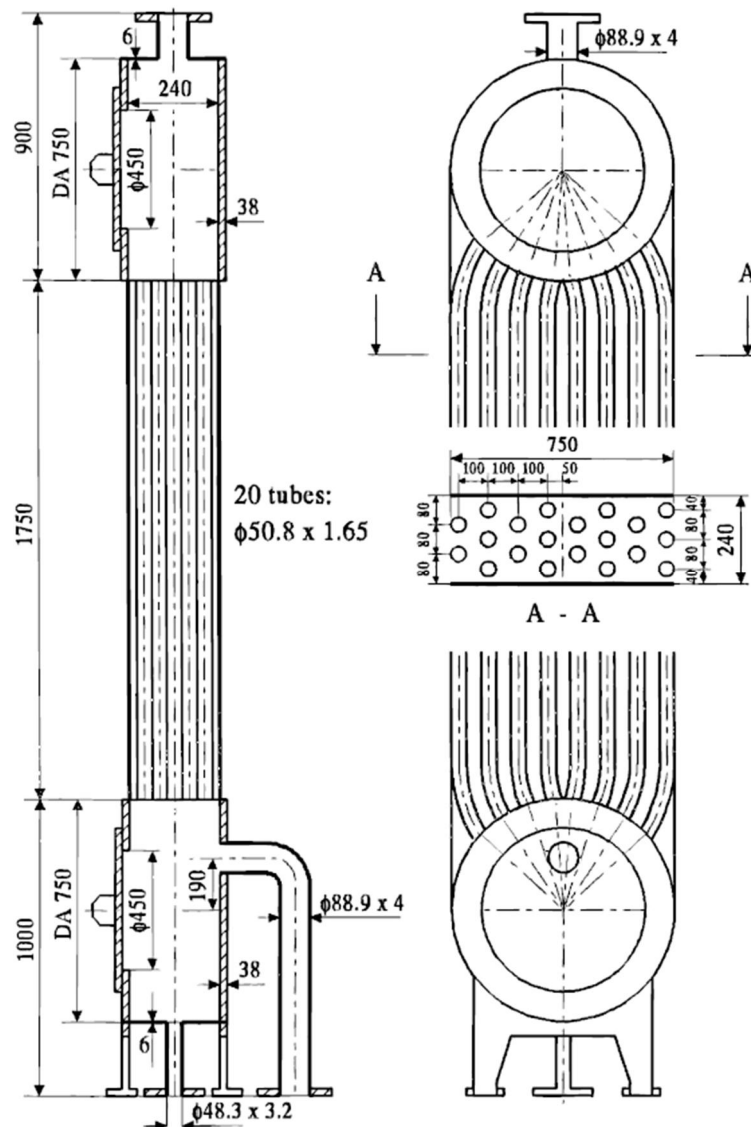


Fig. 7. PANDA PCC unit (Stempniewicz 2000).

The first experiments, so-called S-series, were conducted in 1995 to investigate the steady-state operation of a PCC. In these tests, steam and air were injected directly into the upper header. So, these were not passive tests. The liquid drain flow was discharged into a pool, and the vent flow was directed to an empty wetwell. So, the end of the vent pipe was not submerged, as it would be in the plant. In pure steam tests the vent line was closed. The pressure in these tests was about 3 bar, and the air mass fraction was varied between 0 and 12.4 %. For most of the tests the steam flow rate was about 0.19 kg/s, but also 0.26 kg/s pure steam flow was tested. The secondary side contained boiling water at atmospheric pressure. In one pure steam test, the secondary side water level was lowered to the bottom of the upper header. Stempniewicz (2000) has published data that seems to be sufficient for simulating seven S-series steady-state tests with a computer code. Similar steady-state tests have also been conducted in the B-series (Faluomi & Aksan 1998). In addition to pure steam and air-steam tests, the B-series also included helium-steam tests.

The full PANDA facility that has been used in integral experiments is shown in Fig. 8. It represents the SBWR containment at 1:25 scale, or the ESBWR containment at 1:40 scale.

The most important heights are approximately the same as in the plant. The facility consists of six large vessels. One of them represents the reactor pressure vessel (RPV), which acts as a steam source. Heater rods with maximum total power of 1.5 MW are located at the bottom of the RPV.

The containment drywell is simulated with two cylindrical vessels, D1 and D2 in Fig. 8. They are 8 m high, and their volume is 89.9 m<sup>3</sup> each. They are connected to each other by a 1 m diameter pipe. The containment suppression chamber (wetwell), is simulated with two cylindrical vessels, S1 and S2. They are 10.11 m high, and their volume is 115.9 m<sup>3</sup> each. They have about 4 m deep water pools. They are connected to each other by two pipes. A pipe with 1.5 m diameter connects the water pools, and a pipe with 1 m diameter connects the gas spaces. (Lübbesmeyer & Aksan 2003)

The RPV is connected to the drywells by two main steam lines (MS1 and MS2 in Fig. 8). Both drywells are connected to the suppression chambers by main vent lines, whose lower ends are submerged. In addition, the gas spaces of the same vessels are connected by vacuum breakers (VB1 and VB2). They have valves that open when the suppression chamber pressure exceeds the drywell pressure by a certain margin and reclose when the pressures have equalized. (Lübbesmeyer & Aksan 2003)

The last vessel represents the gravity driven cooling system (GDCS) pool, with a volume of 17.6 m<sup>3</sup> and height of 6.06 m (Lübbesmeyer & Aksan 2003). It is connected to the RPV by the drain line and to the suppression chambers by the pressure equalization line. In the original SBWR configuration, the GDCS was connected to the drywell. The connection to the suppression chambers represents an earlier 4000 MW<sub>th</sub> ESBWR design. In the present 4500 MW<sub>th</sub> ESBWR design, the GDCS is again connected to the drywell (Paladino et al. 2011).

At the top of the facility, there are four rectangular water pools that are open to the atmosphere. Only three of these, housing the PCC units, are shown in Fig. 8. The fourth pool houses an isolation condenser, which was used as a passive core cooling condenser in some experiments. The upper headers of the PCC units are connected to the drywells. PCC1 is connected to D1, and PCC2 and 3 are connected to D2. The drain lines of the PCCs discharge to the RPV. The vent lines are submerged in the water pools in the suppression chambers. In addition to the pipelines shown in Fig. 8, there are several pipelines for gas injections into the vessels.

Eight integral experiments, so-called P-series, were performed in the PANDA facility in 1997–1998. P1 was called the *base case*. It was simulating a long-term cooling phase, starting 1 h after a main steam line break. Steam was injected to both drywells, and all three PCC units were in operation. P8, *PCC pool boil down* test was an extension of P1. It allowed the water levels in the PCC pools to decrease, investigating the operation of partially submerged condensers. P2 *early start* test was simulating the conditions at 20 min after a main steam line break, starting with GDCS injection to the RPV. (Hart et al. 2001)

P3 *PCCS start-up* test demonstrated the PCC start-up in challenging conditions, where the drywells were initially filled with air. Only PCC units 2 and 3 were operational, and steam was injected only to drywell 2. Drywell 1 acted as a dead-end volume. P4 *trapped air in DW* test was started in a similar way as P1 test and confirmed the reproducibility of the tests. After 4 h, air was released into drywell 1 for a period of 30 min, in order to investigate the effect of non-condensable gas on the PCC operation. (Hart et al. 2001)

P5 *symmetric case* was performed with PCC2 disconnected. Later in the transient, air was released to drywell 1. In P6 *systems interaction* test, an isolation condenser was used as a core cooling device, connected to the RPV. In addition, all three PCC units were operational. A

leak path between drywell 1 and wetwell 1 was opened after 4 h, but it did not have a large effect because the pressures of these vessels were almost equal. (Hart et al. 2001)

P7 *severe accident* test was made with PCC 1 disconnected and steam supply only to drywell 2. Between 4 and 6 h, helium was injected to the top of the dead-end volume drywell 1. This simulated the release of hydrogen from zirconium oxidation. 1 h after the start of the helium injection, the helium reached drywell 2, causing a degradation of the PCC performance and therefore an increase of pressure. (Hart et al. 2001)

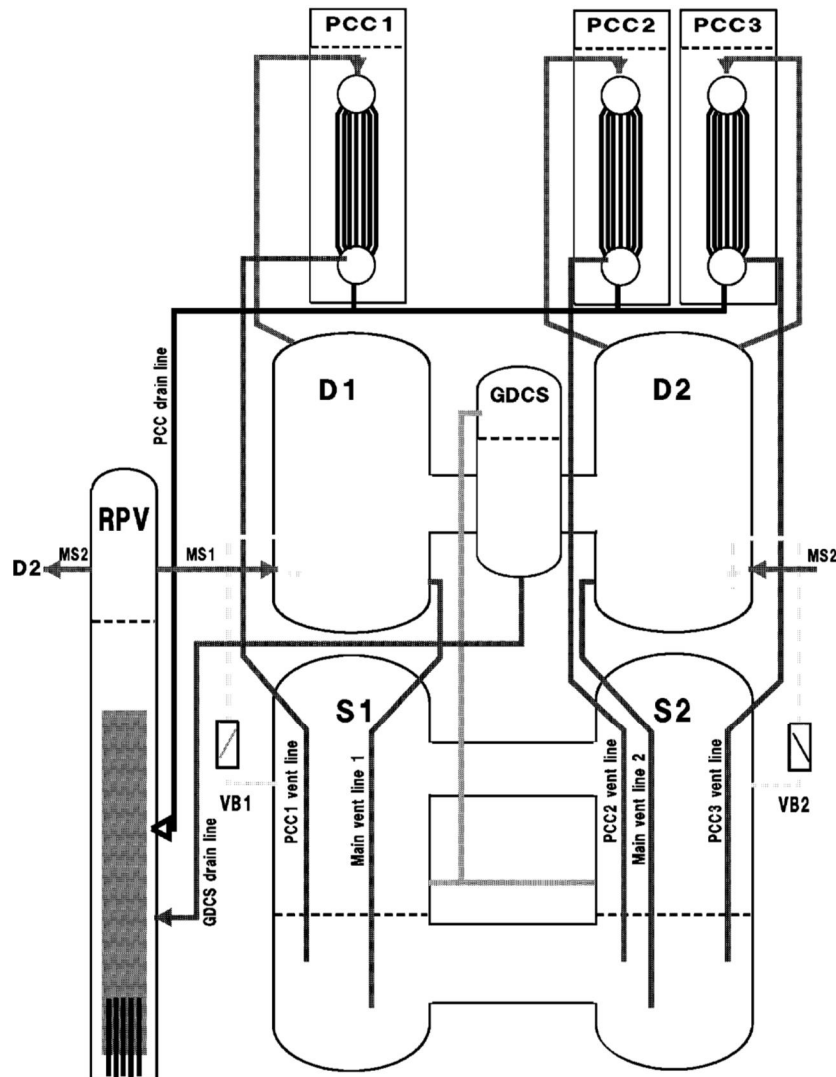


Fig. 8. The PANDA facility (Lübbesmeyer & Aksan 2003).

PANDA ISP-42 test was performed in April 1998. It consisted of six phases, A to F. Each phase is actually a separate experiment with its own initial and boundary conditions. ISP-42 phase A, *PCC start-up*, investigated the startup of the PCCs when steam was injected into the cold vessels filled with air. All three PCC units were operational, but the main vent lines and the vacuum breaker lines were not operational. Phase B, *GDCS discharge*, investigated discharge of cold water into a saturated RPV. The drywells were initially filled with steam. All three PCC units and the vacuum breaker lines were operational, but the main vent lines were not operational. Phase C, *normal operation in case of LOCA*, investigated the long-term decay heat removal from the containment with three PCCs operating. The RPV heating power was gradually decreased, following a decay heat curve. The main vent lines and the vacuum breakers were operational. (Lübbesmeyer & Aksan 2003)

ISP-42 phase D, *PCC overload*, investigated the operation of the PCC system in case of overload at pure steam conditions. Only two PCC units, both connected to drywell 2, were operational. Steam flow from the RPV was directed to drywell 2 only. Therefore drywell 1 and wetwell 1 worked as dead-end volumes. The heating power was higher than the capacity of the two PCC units. The main vent lines were operational but the vacuum breakers were not operational. In phase E, *release of trapped air*, the facility configuration was the same as in phase D, but the heating power was smaller. Air was injected to the top of drywell 1. Phase F, *severe accident*, investigated the release of helium into the RPV. PCCs were not operational in this phase. (Lübbesmeyer & Aksan 2003)

Paladino et al. (2003a) have published information about three PANDA experiments, T1.1, T1.2 and T1.3. For these tests, performed in 2002, a mass spectrometer was added to the test facility, allowing measurement of gas concentrations in 27 locations in the drywells, their interconnecting pipe, and in the wetwells. Test T1.1, *base case*, simulated a main steam line break with all three PCC units operational. Test T1.2, *stand-by volume case*, had only PCC units 2 and 3 operational, and the inflow was directed to drywell 2 only. The vent line from drywell 1 was closed. Test T1.3, *asymmetric case*, used also PCC units 2 and 3 only, but the inflow was directed to drywell 1 and the vent line from drywell 2 was closed. Helium was released along with steam to the drywells in all three tests. It was observed that the flow direction can reverse in some of the PCC tubes. This is probably caused by the decrease of the density of the steam–helium mixture when the steam condenses.

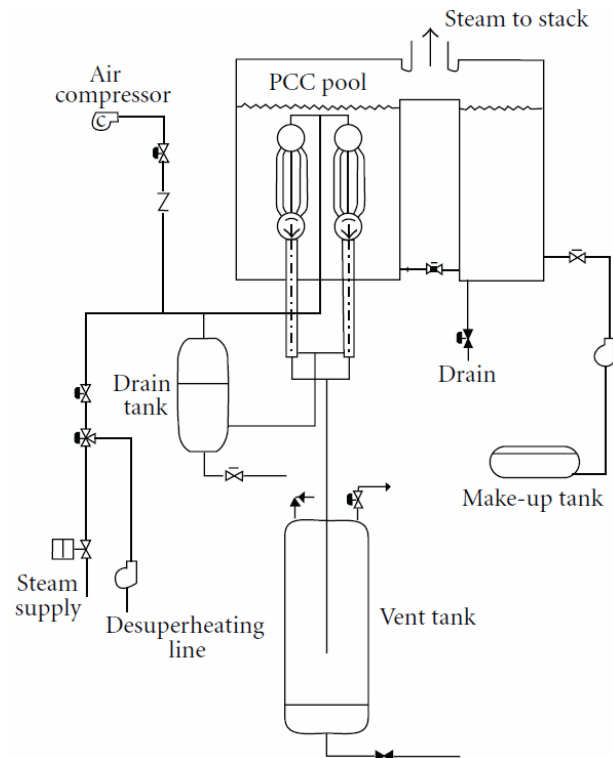
Auban et al. (2003) describe T2.1 and T2.2 experiments. The difference to T1.1–1.3 tests was that a DGRS (Drywell Gas Recirculation System) was activated. DGRS has a fan that feeds some of the PCC vent flow back to the drywell instead of discharging all to the wetwell. DGRS caused slightly lower pressures than a corresponding experiment without DGRS.

In 1996–1998, the SWR-1000 (nowadays called Kerena) containment cooling condenser (Fig. 1) was tested in PANDA BC experiments. In this configuration, the PANDA facility simulates the SWR-1000 containment at 1:26 scale. 25 finned tubes were placed in the drywell 1 vessel. Cooling water came from a pool at an upper elevation, flowed passively through the inclined condenser tubes and returned to the pool. Six experiments, BC1–BC6, were performed. They involved injecting steam or helium to various locations in the vessels. (Dreier et al. 1999)

#### 2.1.6 PANTHERS Experiments

PANTHERS (Performance Analysis and Testing of Heat Removal Systems) experiments have been performed at SIET in Italy. They used a full-scale SBWR passive containment cooling system condenser. However, the condenser was not used in the passive mode. Instead, steam and air were actively fed into the condenser.

The PANTHERS PCC facility is illustrated in Fig. 9. There was one full-size condenser unit, while there are three units in an SBWR plant. One unit consists of two modules, each of them containing 248 tubes. The tubes were 1.35 m long and had 50.8 mm outer diameter. The tubes were connected to upper and lower headers. Steam and air was fed to the upper header. The condensed water flowed from the lower header to the drain tank. Air and uncondensed steam flowed to the vent tank. The vent tank simulated the suppression chamber of the SBWR, but the vent pipe was not submerged in the experiments, while in the plant it would be under water. Several test series were conducted at various pressures, flow rates and air concentrations. The same facility has also been used for testing of an isolation condenser, which removes decay heat from the reactor core. (Ambrosini et al. 2009; Parlattan et al. 1996)

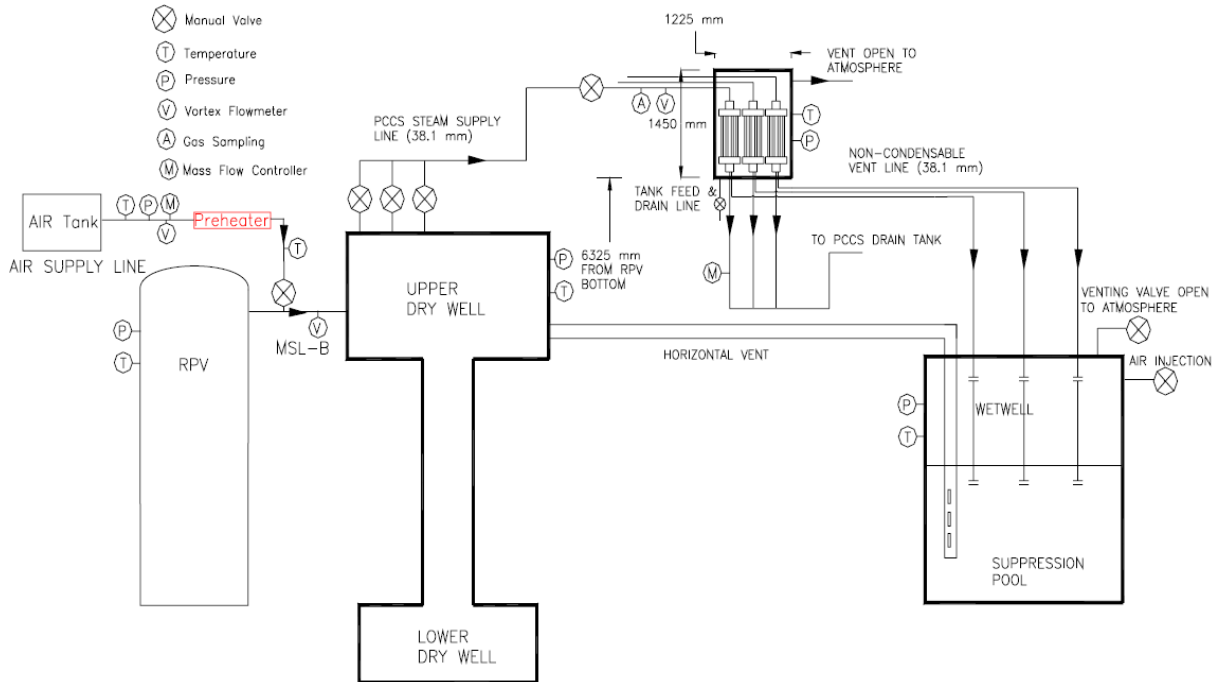


*Fig. 9. PANTHERS PCC facility (Ambrosini et al. 2009).*

### 2.1.7 PUMA Experiments

PUMA stands for Purdue University Multi-Dimensional Integral Test Assembly. It simulates the SBWR PCCS with height scaling 1:4 and volume scaling 1:400. A drawing of the PUMA facility for PCCS separate effect tests is shown in Fig. 10. Steam and air were injected into the upper drywell. There were three PCCS units, each having 10 active tubes. The wetwell was connected to the PCCS and to the upper drywell by vent lines. In the separate effect tests, the wetwell pressure was controlled by air injection and venting to the atmosphere. Dozens of tests have been conducted with various steam flow rates, pressures, pool water levels and air concentrations. (Ishii et al. 2007)

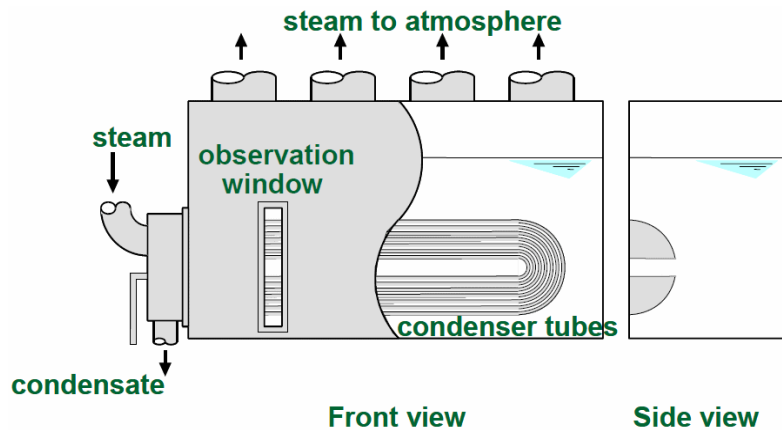
In integral tests in the PUMA facility, an isolation condenser system (ICS) for cooling the core was also used, in addition to the PCCS. Liao et al. (2008) have published an article on MELCOR assessment against a PUMA main steam line break test, which was conducted in 1998. In the long term, the measured pressure leveled off because the heat removal from the containment became equal to the heat injection. However, MELCOR calculated a slowly increasing pressure trend because it underestimated the heat removal especially in the ICS. Consequently, MELCOR calculated too large steam release rate to the drywell and therefore too large flow rate through the PCCS. This, in turn, caused continuous venting of uncondensed steam to the wetwell in the calculation, which differs from the test result.



**Fig. 10.** PUMA facility for separate effect PCCS tests (Ishii et al. 2007).

### 2.1.8 ROSA/LSTF Experiments

A horizontal tube PCCS, where the condensation takes place inside the tubes, has been tested in the ROSA/LSTF facility at Japan Atomic Energy Agency (JAEA). The tube bundle was full-scale but halved, as shown in Fig. 11. The tube length was 8 m. The steam feed was active, i.e. these were not passive experiments. (Ishii et al. 2007; Kojima et al. 2010)

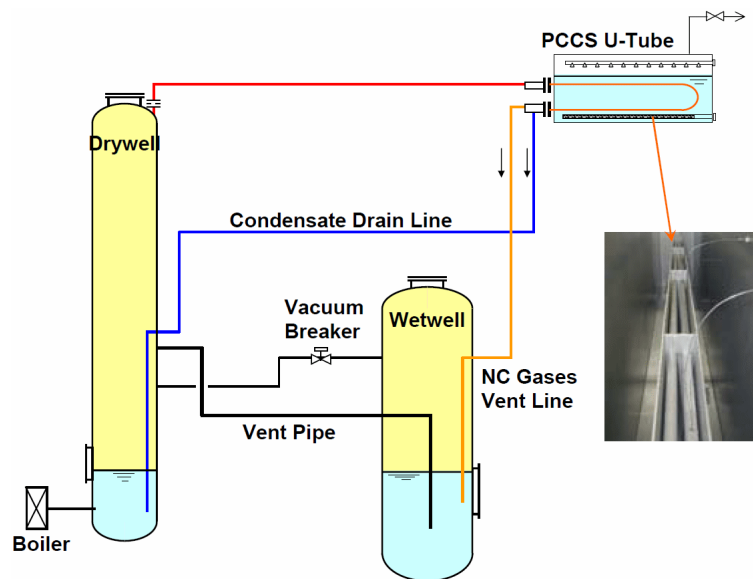


**Fig. 11.** Japanese test facility for a horizontal PCCS (Ishii et al. 2007).

The Japanese have also measured steam condensation in the presence of non-condensable gases in a single horizontal U-tube (Arai et al. 2002; Kondo et al. 2002; Ishii et al. 2007). The tube was cooled by subcooled water flowing in cooling jackets. Modeling steam condensation in a horizontal tube appears more difficult than in a vertical tube because the cylinder symmetry is lost. In a vertical tube all the sides are identical, but in a horizontal tube the condensate film is thicker at the bottom of the tube than at the top. Therefore heat transfer at the top of a horizontal tube is more efficient.

### 2.1.9 TIGER Experiments

Toshiba has made integral system tests with a horizontal PCCS where the condensation takes place inside the tubes. The TIGER (Toshiba Innovative Geminant Test Loop for Reactor Safety System) facility has two U-shaped heat exchanger tubes, 8 m long, immersed in a water pool (Fig. 12). The upper end of the tubes was connected to a vessel simulating the drywell, which contained steam and non-condensable gases. The condensate was returned to the drywell through a drain line, and the gases were vented to a wetwell vessel. The drywell and wetwell were connected by a vent pipe and a vacuum breaker. Thus, both primary and secondary sides of the TIGER facility were passive. (Kojima et al. 2010)



*Fig. 12. TIGER test facility for horizontal tube PCCS integral testing (Kojima et al. 2010).*

### 2.1.10 Summary of Passive Containment Condenser Experiments

A large amount of experimental data exists about heat transfer in passive containment condensers. The ESBWR condenser appears the most extensively tested. Scaled integral experiments have been performed in the PANDA and PUMA facilities and non-passive full-scale tests in the PANTHERS facility. Also the Kerena condenser has undergone lots of testing in the INKA and PANDA facilities and separate effect tests in the NOKO facility. The AES-2006 condenser is said to be similar to the Kerena condenser, so the same experiments may be applicable also for this Russian reactor design. Simulating the horizontal ABWR condenser is more challenging due to the loss of cylinder symmetry. Some experiments on horizontal tube PCCS have been conducted in the ROSA/LSTF and TIGER facilities.

An interesting observation was the flow reversal in the PANDA T1.1–1.3 experiments where helium was mixed with steam. This makes it more challenging to simulate the ESBWR type condenser behavior in the presence of a light gas.

## 2.2 Experiments on Aerosol Deposition in Condensers

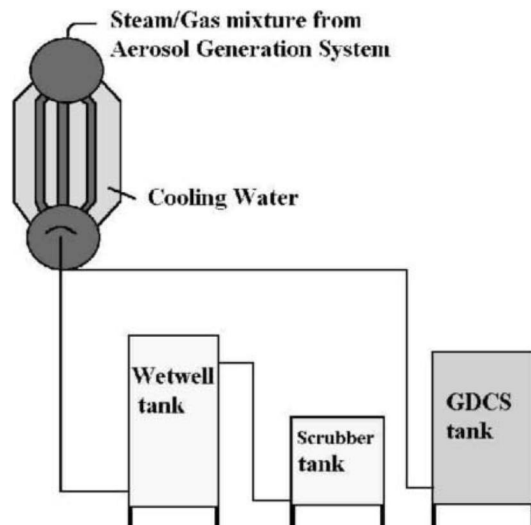
Aerosols would be released to the containment atmosphere in a severe accident. Some of the aerosols would be drawn into the condenser, where they can form deposits. This could have a negative effect if the deposits block the flow in the condenser or decrease the heat transfer efficiency. On the other hand, if the condenser removes aerosols from the containment atmosphere, radioactive emissions to the environment can decrease. In addition, the decay



heat that is generated by the deposited aerosols may have an effect on the operation of the condenser.

### 2.2.1 AIDA Experiment

One PCCS experiment has been performed in the AIDA (Aerosol Impaction and Deposition Analysis) facility at PSI, Switzerland. The facility is shown in Fig. 13. Steam, non-condensable gases and SnO<sub>2</sub> aerosols were injected into a condenser that works with the same principle as the ESBWR condenser. The cooling water flowed at the secondary side under forced convection. So, the AIDA experiment was not passive. Significant aerosol deposition took place, and the heat transfer degradation reached 20 %. (Hart et al. 2001)

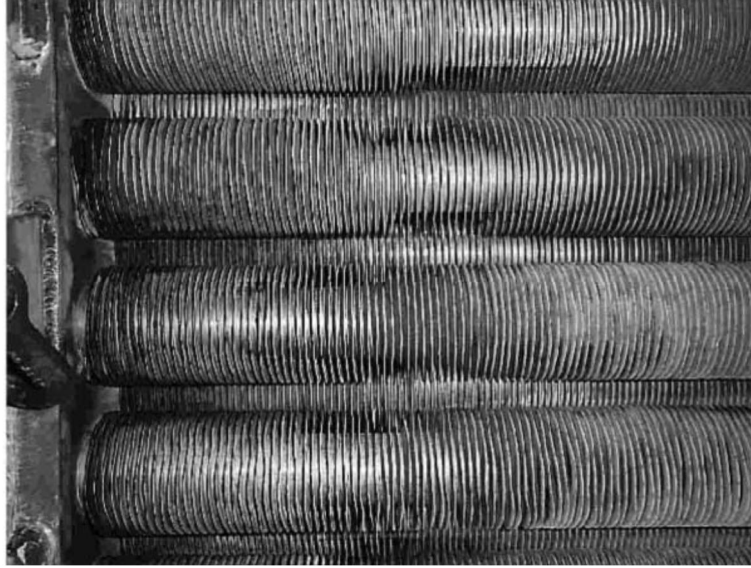


*Fig. 13. AIDA experimental facility (Hart et al. 2001).*

### 2.2.2 CESANE and STORM Experiments

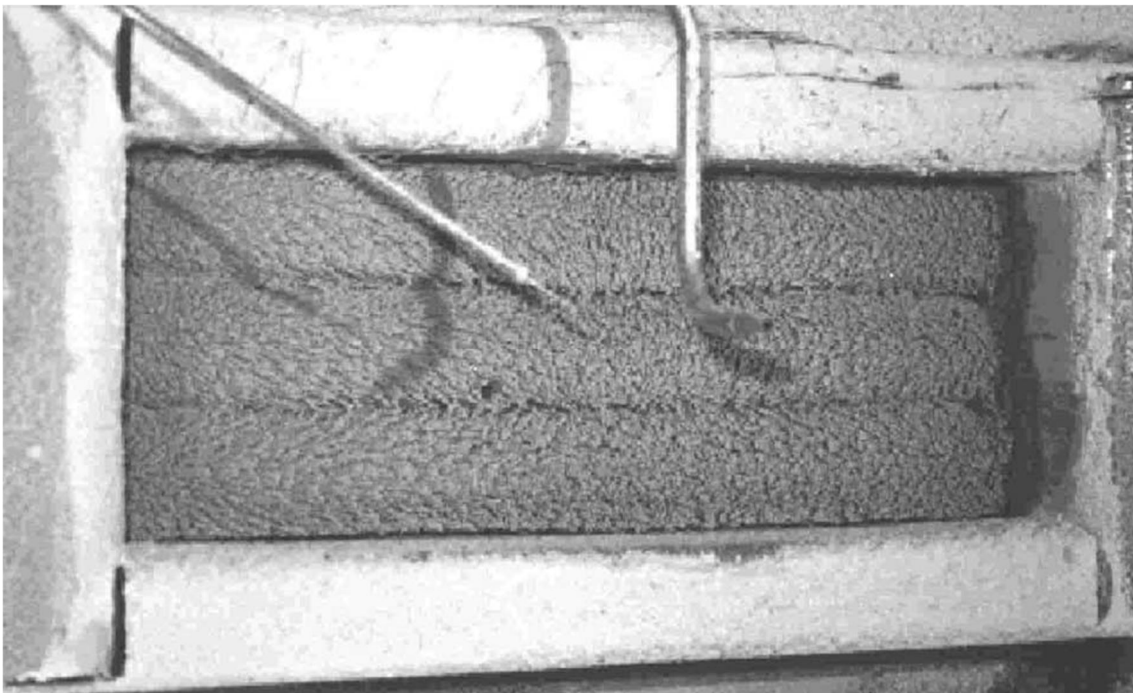
Heat transfer and aerosol deposition on horizontal finned tubes was examined in CESANE (Condensation Experiments in Steam Aerosol Non-condensable Environment) experiments at PSI, Switzerland, and in STORM experiments at JRC, Italy. Condensation took place on the outer surface of the tubes, so the principle is the same as in the Kerena reactor design (Fig. 1). These tests are combined into a single section in this report because they were similar. Both have been reported by Friesen et al. (2001).

Cooling water was pumped through the tubes. Flow of steam, non-condensable gases, and SnO<sub>2</sub> and CsOH aerosols was directed to the tube bundle from the top. Thus, these were not passive experiments. Tube dimensions and their detailed geometric configuration have not been published in the available literature. A photo of the tubes in the STORM facility is shown in Fig. 14.



**Fig. 14.** Condenser tubes in the STORM facility (Friesen et al. 2001).

Despite the similarity of the CESANE and STORM experiments, their results differ significantly. In the CESANE experiments, substantial aerosol deposition was observed (see Fig. 15). The heat removal rate was reduced by 7–37 % compared to clean tubes. On the contrary, in the STORM experiments only very small amounts of deposited material were found, and no degradation of the heat removal rate was observed. According to Muñoz-Cobo et al. (2005), the reason for the difference was probably smaller gas flow velocities in the STORM experiments, making impaction deposition mechanism non-effective. Also the different geometrical arrangement of the tubes may play a role.



**Fig. 15.** Condenser tubes in the CESANE facility after an experiment (Friesen et al. 2001).

### 2.2.3 Gröhn et al. Experiments

Gröhn et al. (2009) have performed experiments on aerosol deposition in a condensing heat exchanger at University of Kuopio, Finland. The heat exchanger consisted of 121 vertical

tubes with inner diameter of 8 mm and length of 745 mm. Exhaust gases from a wood-burning stove flowed downwards through the tubes. Cooling water was pumped upwards outside the tubes. The gas temperature was 137–175 °C before the condenser and 24–61 °C after the condenser. The gas contained about 40 nm particles, and its humidity was 5–29 % by volume. The number of particles decreased by 25–41 %. The median particle size increased slightly. These results include the effect of agglomeration. The deposition increased along with an increase in the humidity or in the inlet gas temperature.

#### 2.2.4 Lehtinen et al. Experiments

Lehtinen et al. (2002) have performed experiments on steam condensation and aerosol deposition in a vertical heat exchanger tube. The facility was simply a vertical tube with 22 mm inner diameter and 1.5 mm wall thickness. Steam, nitrogen and aerosols were injected into the tube, flowing downwards. The tube was surrounded by a cooling jacket. Water flowed upwards in the jacket at 2.8 L/min. The water inlet temperature was 11.6 °C. The length of the cooled area was 85 cm. The aerosol concentration was approximately 0.1 g/m<sup>3</sup>, and aerodynamic mass mean diameter (AMMD) was about 1.0 µm. The measured quantities included gas temperature at the tube outlet, condensation rate and aerosol deposition rate.

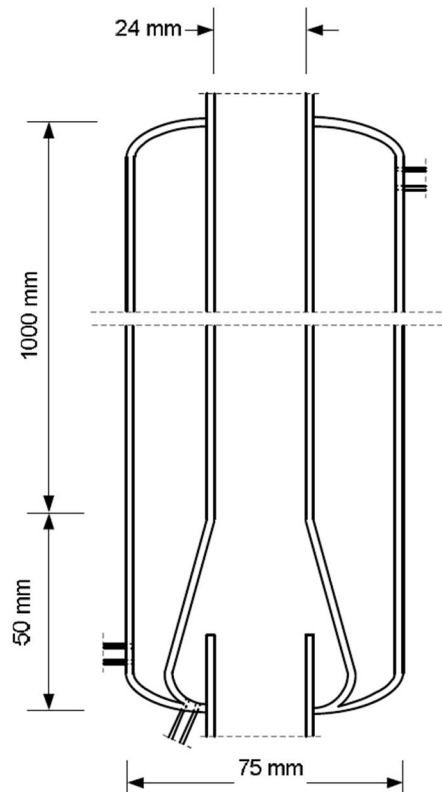
Three steady state experiments were published by Lehtinen et al. (2002). Their boundary conditions and results are shown in Table 1. The *dry* and *low steam* experiments were done with Ag particles only. The *high steam* test was made with both pure Ag and Ag + CsOH particles. The deposition losses were 52.8 and 53.4 %, respectively. Thus, the aerosol material did not affect the deposition rate in this experiment. Since the measured aerosol size distribution did not change during any of the experiments, it is concluded that the particle size had only a very minor effect on the deposition rate. In the experiments with steam, most of the deposited material was washed off by the condensed water. So, the deposition did not affect the heat transfer rate. In the dry experiment the deposition was too small to cause any deterioration in the heat transfer.

**Table 1.** Boundary conditions and results of three experiments by Lehtinen et al. (2002).

Test name	Dry	Low steam	High steam
N <sub>2</sub> flow rate (L/min, NTP)	100	75	25
Inlet steam flow rate (g/min)	0	18.4	60.5
Inlet gas temperature (°C)	205	207	203
Outlet gas temperature (°C)	116	129	150
Condensation rate (g/min)	0	9.5	43.3
Deposition (particle loss %)	4.3	17.2	53

#### 2.2.5 Suonmaa Experiments

Suonmaa (2006) has performed experiments on aerosol deposition in a condensing heat exchanger at University of Kuopio, Finland. Exhaust gases from a wood-burning stove were led upwards through the inner tube (Fig. 16). Cooling water was pumped upwards between the tubes. The length of the uniform condenser tube was 100 cm. At the bottom of the tube there was a condensate collector, 5 cm high. The gas temperature was around 140 °C before the condenser and slightly over 60 °C after the condenser. The gas contained about 40 nm particles. About 7.5 % of the mass of the particles was deposited in the tube. The reason for the small deposition was the low humidity, about 4 % by volume, in the incoming gas. The small deposition did not cause heat transfer rate deterioration. The particle size distribution did not change in the heat exchanger.



*Fig. 16. Condensing heat exchanger used in the Suonmaa (2006) experiments.*

### 2.2.6 Summary of Experiments on Aerosol Deposition in Condensers

Scarce experimental data on aerosol deposition in condensers was found in the published literature. For the Kerena-type condenser, the CESANE and STORM experiments produced very different results, despite the similar geometrical arrangements. Sufficient details of the experiments have not been published, so it is not possible to use them for computer model validation.

For the ESBWR-type condenser, the Lehtinen et al. experiments provide three well-reported tests about particle deposition in a vertical condenser tube. They offer some data for validating deposition models but not for developing heat transfer deterioration models. The AIDA experiment might complement the Lehtinen et al. tests as regards the heat transfer degradation issue, but the AIDA results have not been published in sufficient detail. The AIDA test was just a single experiment, so it does not provide information about the effect of the various boundary conditions on the results.

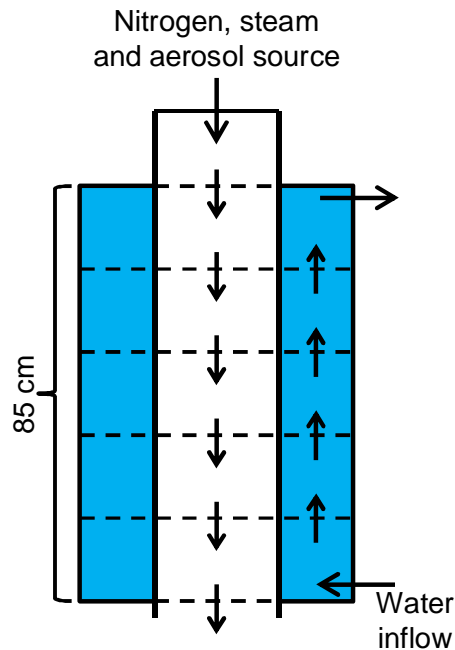
## 3 MELCOR Modeling of Lehtinen et al. Condensation and Aerosol Deposition Experiments

In (Sevón 2010), Purdue University experiments on steam condensation in a vertical tube in the presence of non-condensable gases were simulated with MELCOR. It was concluded that, with the default parameters, MELCOR underestimates the condensation rate by about 20 %, both with pure steam and steam–air mixtures. The problem was solved by changing the condensate film Reynolds number limits, for classifying the film flow as laminar or turbulent, from the default values of 1000 and 3000 to the values recommended by Incropera & DeWitt (2002): 30 and 1800.

The Purdue University experiments (Oh 2004) were limited to air concentrations below 8.9 mass-% at the inlet (max. 16 mass-% at the outlet). In this chapter, the condensation validation database is extended to higher non-condensable gas concentrations (34–100 mass-%) by simulating the Lehtinen et al. (2002) experiments, which were described in section 2.2.4. Also the aerosol deposition in the experiments is compared with the MELCOR results.

### 3.1 Model

The nodalization that was used in the MELCOR simulations of the Lehtinen et al. experiments is shown in Fig. 17. The 85 cm long water-cooled tube section was divided into five control volumes inside the tube and five control volumes in the cooling jacket. In addition, there was an inlet volume at the top of the tube, where nitrogen, steam and aerosols were injected as mass sources. A time-independent control volume was defined for simulating the environment, receiving outflows from the bottom of the tube and from the top of the cooling jacket. The flow path out from the cooling jacket was a *forward only* path in order to prevent gas flow into the cooling jacket.



**Fig. 17.** MELCOR nodalization of the Lehtinen et al. experiments. The dashed lines are control volume boundaries.

It is important that the mass sources are not defined directly to the active part of the tube because, when calculating flow velocity in a control volume, MELCOR takes into account only flow paths but ignores mass sources (Sandia 2011, equation 6.20). Therefore MELCOR underestimates flow velocity in a volume that has a mass source. This would underestimate heat transfer coefficients if a heat structure is interfaced with such volume. This is the reason for using the additional inlet volume at the top of the tube. For the cooling jacket, the same problem was avoided by injecting the water through a time-dependent flow path instead of a mass source. The “from” volume of this flow path was a time-independent control volume that is not shown in Fig. 17.

There were five heat structures simulating the tube wall, made of stainless steel. The tube diameter 22 mm was used as the characteristic length on the inner side of the structure. On the outer side, the characteristic length was set to 5 mm, which is the width of the gap where the water flows. A film tracking network was defined to model the condensate film flow along

the inside of the tube. An additional auxiliary heat structure was defined for receiving the condensate from the lowermost active heat structure and draining the water to the environment volume. The only objective of this auxiliary structure was to avoid formation of a tiny water pool at the bottom of the lowermost control volume because it would cause oscillation in the simulation. This auxiliary structure was defined inactive for aerosol deposition, so it did not affect the calculated deposition.

The condensate film Reynolds number limits, for classifying the film flow as laminar or turbulent, were changed from the default values of 1000 and 3000 to the values recommended by Incropera & DeWitt (2002): 30 and 1800. This has been found to significantly improve MELCOR's condensation modeling results with small non-condensable gas concentrations (Sevón 2010).

### 3.2 Results

The three experiments were simulated with MELCOR 2.1 revision 3226. The calculation was run for 1000 s to make sure that equilibrium has been reached, and the results were taken from the end of the calculation. They are compared with the measurements in Table 2. The boundary conditions of the experiments were given in Table 1. The condensation rate is calculated correctly for the *low steam* test and underestimated by 8 % for the *high steam* test. Lehtinen et al. (2002) do not give measurement uncertainties, but 8 % difference is considered to be a good result. Heat transfer in the *dry* test can be assessed by comparing the gas outlet temperature. MELCOR result was 114 °C, and the measurement was practically the same, 116 °C.

Aerosol deposition is slightly overestimated in the *dry* test and somewhat underestimated in the two tests with steam. MELCOR correctly calculates that the aerosol size distribution was practically the same in the inlet and outlet of the tube.

**Table 2.** MELCOR results of three experiments by Lehtinen et al (2002), compared with the measurements.

Test name	Condensation rate (g/min)		Deposition (particle loss %)	
	Measured	MELCOR	Measured	MELCOR
Dry	0	0	4.3	5
Low steam	9.5	9.4	17.2	11.5
High steam	43.3	39.8	53	43.2

The effect of nodalization was investigated by calculating the *high steam* test with fewer control volumes. The results (Table 3) diverge from the measurements when the number of control volumes is decreased, but the difference between three- and five-volume models is only 1.3 %. Three control volumes would have been sufficient for this experiment. Even the one-volume model is not bad, deviating 5 % from the three-volume model.

**Table 3.** Effect of nodalization on the MELCOR results of the high steam test.

Control volumes for active tube length	Condensation rate (g/min)	Deposition (particle loss %)
5	39.8	43.2
4	39.6	43.0
3	39.3	42.6
1	37.2	40.2
Measured results	43.3	53

When calculating the Purdue university experiments, Sevón (2010) found out that the difference between one- and three-volume models was only 2 % for the one meter long tube. The reason for the larger difference in the Lehtinen et al. experiments is that they had a more difficult boundary condition. The Purdue experiments had boiling water outside the tube, so the boundary condition was uniform. The Lehtinen et al. experiments had flowing subcooled water on the outside, so the water was warmer at the upper end of the tube. This variation of the boundary condition requires a more detailed nodalization.

The results reported above were calculated using the modified condensate film Reynolds number limits. For comparison, the calculations were repeated with MELCOR's default Reynolds number limits. The results were practically the same, with max. 0.2 % difference. This finding differs from the Sevón (2010) calculations of the Purdue university experiments, where modifying the Reynolds number limits was found to improve the results significantly. The reason is that in the Lehtinen et al. experiments, the film Reynolds number was mostly below 30 and may have exceeded 30 only in the lower end of the tube in the *high steam* test. Thus, the condensate film was almost completely in the laminar flow regime even with the modified Reynolds number limits. On the contrary, the Purdue experiments had film Reynolds numbers around 100, which is in the transition to turbulence regime with the modified settings but in the laminar regime with the default settings.

## 4 MELCOR Modeling of PANDA T1.1 Experiment

PANDA T1.1 experiment was chosen to be modeled with MELCOR because of its advanced instrumentation and also because the vessels remained quite well mixed during this test. Absence of strong stratification allows concentrating on PCC modeling and avoids difficulties due to stratification modeling with a lumped parameter code.

The model was based on the following documents: Lübbesmeyer et al. (1999), Huggenberger et al. (2002) and Paladino et al. (2003b). In addition, measurement data of the experiment was available. The measurements were made at 2 s intervals. All measurement data that is shown in this report has been smoothed by calculating 30 s averages, so that 15 measured data points are averaged into one point in the plots. This reduces oscillation in the measured curves and makes the plots more readable. The duration of the experiment was 11 h 40 min 8 s.

The main focus of the project was in modeling the passive containment condensers (PCCs). But proper modeling the vessels and pipelines was important for getting the right boundary conditions for the PCCs. The MELCOR model has 104 control volumes, 176 flow paths and 163 heat structures. Section 4.1 describes how the vessels and their connecting pipelines were modeled. The PCC modeling is described in section 4.2. Results of the calculations are given in section 4.3.

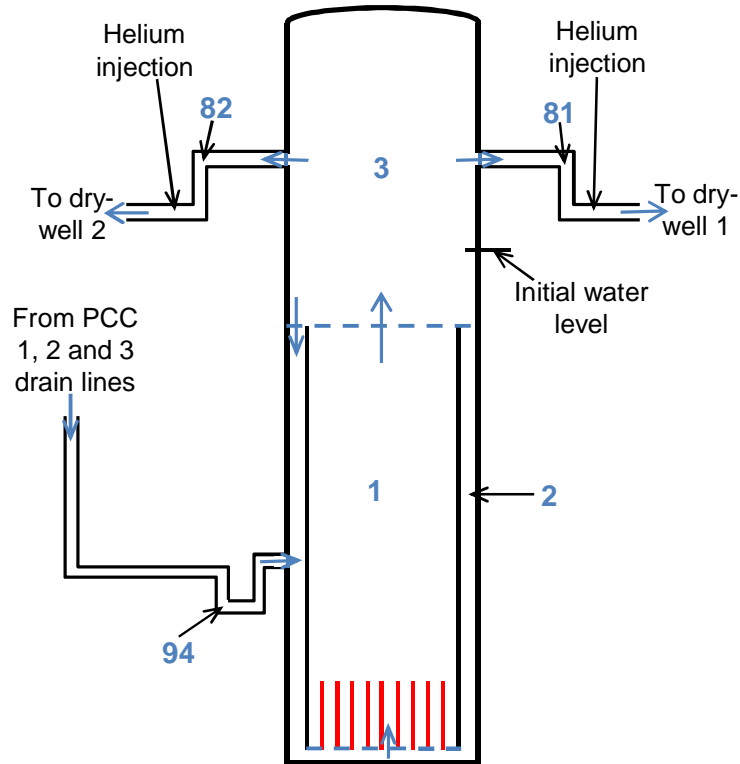
### 4.1 Modeling the Vessels and Pipelines

A general drawing of the whole facility was shown in Fig. 8. A single figure showing the nodalization of all the vessels and pipelines would be complex and unclear. Therefore each vessel is discussed in separate sections and figures. Knowledge of the measurement data was utilized for designing the nodalization, but MELCOR parameters were not tuned for getting the correct results.

#### 4.1.1 RPV Vessel

The RPV nodalization is shown in Fig. 18. The vessel was divided into three control volumes. CV 1 is the riser, CV 2 is the downcomer, and CV 3 is the dome. Main steam line 1 was

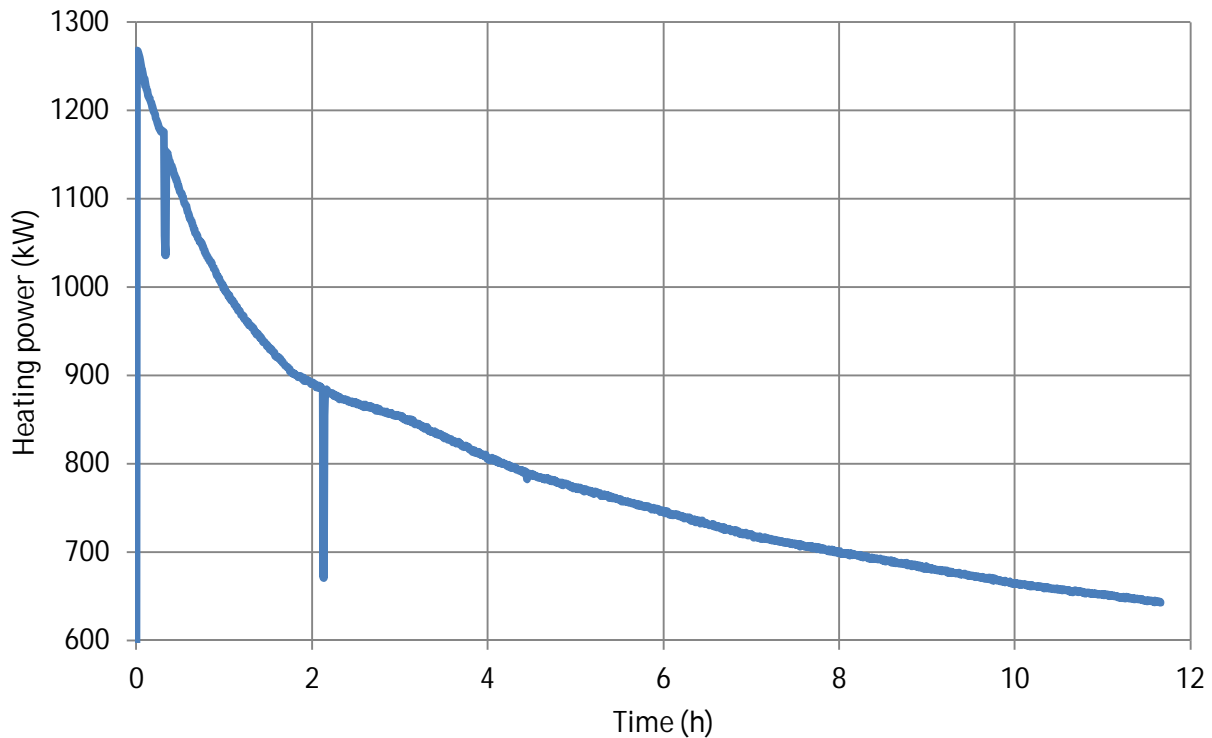
modeled as CV 81 and main steam line 2 as CV 82. The part of the PCC drain lines that is common to all three PCC units is modeled as CV 94. The initial pressure in the RPV dome was 2.66 bar. The temperature was close to saturation, about 129 °C. The bubble rise model was activated in the flow path that goes from the riser to the dome.



**Fig. 18.** Nodalization of the RPV and its connecting pipelines. The blue numbers are control volumes and blue arrows are flow paths. The red lines are the heating rods. The figure is magnified by a factor of four in the horizontal direction to make it more readable. The pipeline lengths are not in the right scale, but pipe elevations are correct.

The heating power in the RPV is plotted in Fig. 19. The curve corresponds to scaled ESBWR decay heat power, starting at 1 h after reactor scram. In the MELCOR model this power was injected to the RPV riser control volume as an enthalpy source in the pool. The helium injection was modeled as mass sources in the steam lines.





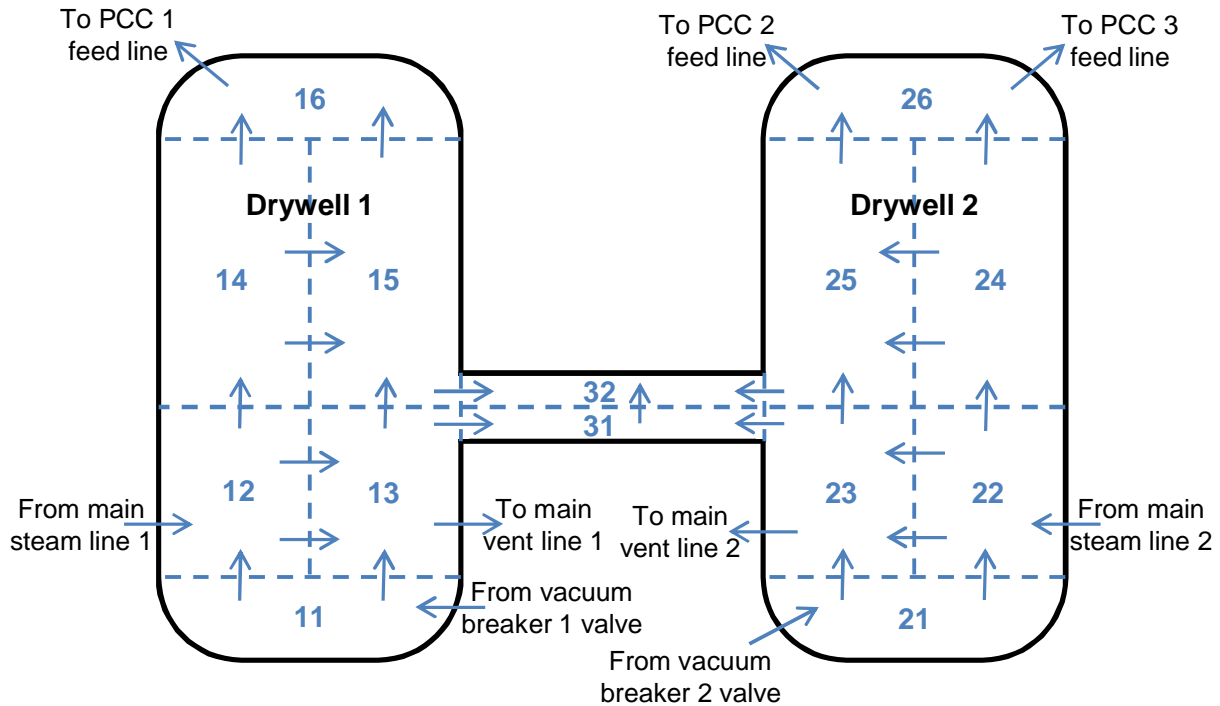
*Fig. 19. Heating power in the RPV.*

#### 4.1.2 Drywells

Nodalization of the drywells and the pipe that connects them is shown in Fig. 20. Both vessels were modeled with six control volumes. They were divided into four axial levels, and the two mid levels were further azimuthally divided into “left” and “right” sides in order to model upwards flow on one side and downwards flow on the other side. The connecting pipe between the drywell vessels was modeled with two control volumes, CV 31 at bottom and CV 32 at top.

The flow paths between the drywell control volumes were modeled with the real geometrical flow areas and center-to-center lengths. The form loss coefficients of the internal flow paths, which do not have sudden changes of flow area, were set to zero. The opening heights of the vertical flow paths were arbitrarily set to 0.1 m. The same convention was followed also in the flow paths of the other vessels. The “left and right side” volumes were connected with two horizontal flow paths between the same control volumes but at different elevations. This allows a two-way natural circulation flow between the adjacent volumes, but it had a negligible effect on the results.

The vacuum breaker lines were not modeled as control volumes because the valves were open only for very brief periods during the experiment. A flow path was defined from wetwell 1 to drywell 1, and another flow path from wetwell 2 to drywell 2. Vacuum breaker valve 1 opened when the wetwell pressure exceeded the drywell pressure by 3.24 kPa and closed when the pressure difference decreased to 2.06 kPa. Vacuum breaker 2 valve would have opened at pressure difference of 3.9 kPa and closed at 2.8 kPa, but this never happened in the experiment. The valve stroke time of 15 s from closed to full open position or vice versa was modeled. (Lübbesmeyer et al. 1999.) For modeling heat loss, the walls of the vacuum breaker pipes were modeled as heat structures whose inner surfaces were interfaced to wetwell and drywell control volumes.



**Fig. 20.** Nodalization of the drywells and the pipe that connects them. Control volumes are marked by blue numbers and their borders are drawn with blue dashed lines. The blue arrows are flow paths.

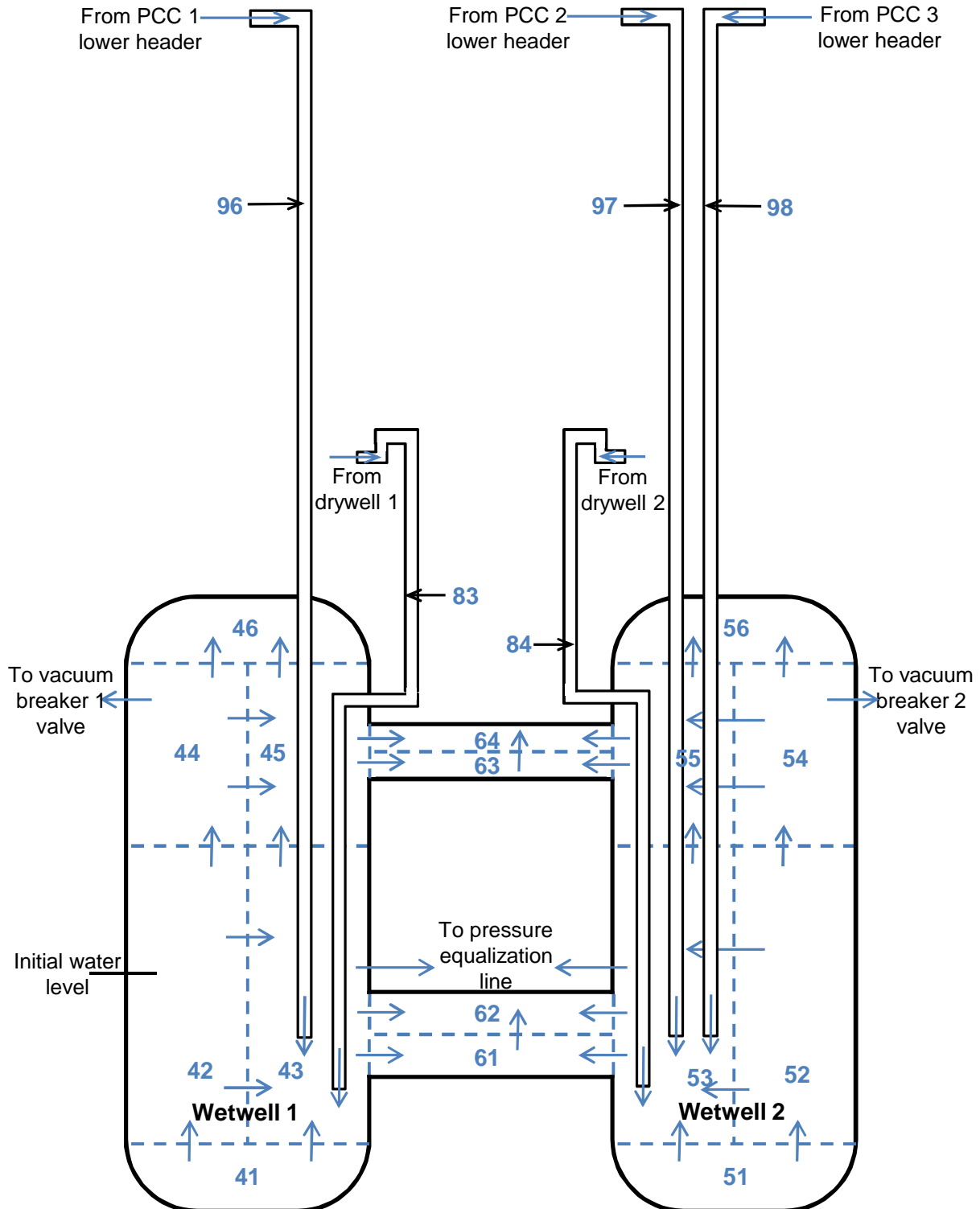
At time zero the pressure in the drywell was 2.54 bar and temperature was about 127 °C. The relative humidity was 100 %, and there was little air in the vessels. There was a very small amount of condensed water at the bottom of both drywell vessels.

#### 4.1.3 Wetwells

Nodalization of the wetwells, the pipes that connect them, and the vent lines, is shown in Fig. 21. Both vessels were modeled with six control volumes. They were divided into four axial levels, and the two mid levels were further azimuthally divided into “left” and “right” sides in order to model upwards flow on one side and downwards flow on the other side. Both connecting pipes between the wetwell vessels were modeled with two control volumes, CV 61 and 62 for the lower pipe below water level, and CV 63 and 64 for the upper pipe above water level.

The main vent line 1 is CV 83 and main vent line 2 is CV 84. The PCC 1, 2 and 3 vent lines are CV 96, 97 and 98, respectively. The elevations in Fig. 21 are drawn to scale. The main vent line pipes were submerged by about 1.88 m and the PCC vent lines were submerged by about 1.03 m. The bubble rise model was activated in the vent flow paths.

At time zero the pressure in the drywell was 2.37 bar, temperature was about 73 °C, and the relative humidity was 100 %. The water level was 3.9 m above the bottom of the vessels.



**Fig. 21.** Nodalization of the wetwell, the pipes that connect them, and the vent lines. Control volumes are marked by blue numbers and their borders are drawn with blue dashed lines. The blue arrows are flow paths.

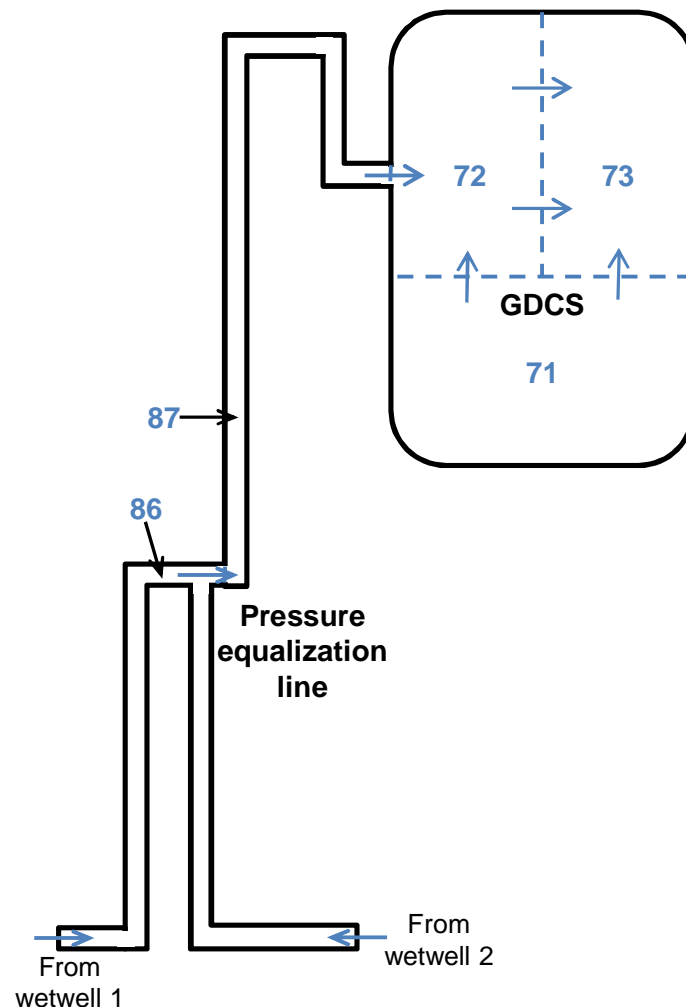
The main vent line valves were closed at 1 h after the start of the experiment and reopened just before helium injection, at 2 h 43 min. In the MELCOR model, the valves were defined in the flow paths leading from the drywell to the vent line. When the valves were closed, steam condensed in the pipes because they were not insulated inside the wetwell vessels. The condensation decreased pressure in the vent lines, which caused the water level to rise very

high in the main vent lines. Opening of the valves returned the water level to the normal value.

#### 4.1.4 GDCS Tank

The GDCS tank acted as a passive volume, effectively increasing the gas volume of the wetwell. It was connected to the gas spaces of both wetwells by the pressure equalization line. There was no water in the GDCS tank in this experiment and the GDCS drain line was closed. Therefore the GDCS drain line was not included in the MELCOR model.

Nodalization of the GDCS tank and the pressure equalization line is shown in Fig. 22. The GDCS tank was divided into three control volumes. So detailed modeling was probably unnecessary because the GDCS was passive during this experiment. The equalization line was modeled as two control volumes. The lower part, which is connected to both wetwells, is CV 86. The upper part, leading to the GDCS tank, is CV 87.



**Fig. 22.** Nodalization of the GDCS tank and the pressure equalization line. Control volumes are marked by blue numbers and their borders are drawn with blue dashed lines. The blue arrows are flow paths.

The initial pressure in the GDCS tank was 2.38 bar and temperature about 57 °C. Gas concentration in the GDCS was not measured. The relative humidity at time zero was set to 100 %, but this is just a guess.

#### 4.1.5 Flow Resistance of Pipelines

Flow resistance of the pipelines determines the flow rate through the PCC units. The flow rate, in turn, affects the heat transfer rate. Proper modeling of the flow resistances is important for correct PCC simulation results.

Lübbesmeyer et al. (1999), section 4.10 gives measured pressure losses at various flow rates for the following pipelines: main steam lines, PCC feed lines and PCC vent lines. The form loss coefficients of these flow paths in the MELCOR model were adjusted so that the calculated pressure drops match with the measurements.

The PCC feed and vent lines had orifices for restricting the flow, in order to get proper scaling of the ESBWR pressure drops. Geometries of the orifices were not described in the available documents, so the measured pressure drops were much larger than what could be inferred from the geometry of the pipelines. This required using quite large form loss coefficients, larger than 10, to match the calculated pressure drop values with the measurements.

#### 4.1.6 Heat Losses from the Facility

The facility was insulated with rock wool. The RPV vessel had 300 mm and the other vessels had 200 mm of rock wool 133 insulation. The pipelines had 100 mm of rock wool 864 insulation. Lübbesmeyer et al. (1999) give the density, heat capacity and thermal conductivity of both rock wool types. These material properties were used when modeling the insulation layers in the heat structures. The outer surface of the heat structures was interfaced with time-independent environment control volume, CV 999, at 20 °C and 0.982 bar. The environment temperature is estimated but the pressure was measured during the experiment.

Lübbesmeyer et al. (1999), section 2.5, gives results of a heat loss test of the facility. The vessels were filled with steam at 4 bar and 140 °C. Then the system was let to cool down for 2.5 days, and the heat loss was measured as a function of temperature. This cool-down test was calculated with MELCOR. There are some uncertainties in the initial conditions. The report does not tell whether there was any water in the RPV or in the wetwells during the cool-down test. In the modeling it was assumed that there was no water and the PCCs were isolated from the system but all other valves in the pipelines were open. Using the specified material properties for the insulation, the heat loss was underestimated by 40 %. The reason for the underestimation is probably that some heat was lost through flanges, auxiliary lines etc. To correct the discrepancy, the specified thermal conductivity of the insulation material was multiplied by 1.6. After this change, the calculated average heat loss differed only 6 % of the measured values. This accuracy was deemed sufficient.

Radiation heat transfer was activated for all heat structure surfaces that were interfaced with other than the environment volume, except for those surfaces that were submerged. The emissivity of the surfaces was set to 0.2. The calculation was made also with the radiation heat transfer switched off. The difference was insignificant. The no-radiation model gave 0.07 % smaller amount of condensation.

#### 4.1.7 Gas Consumption of the Mass Spectrometer

There were 27 gas sampling lines for measuring the gas concentration in the facility. 18 sampling lines were located in the drywell vessels, 3 in the connecting pipe between the drywells, and 6 in the wetwells. Gas was continuously flowing out of the facility through all these sampling lines. This can have an effect on the results.

Paladino et al. (2003b), chapter 7, reports that gas consumption rate of the sampling system was measured as a function of pressure, using pure air and pure helium. However, results of

these measurements were not available to VTT. Paladino et al. (2003b) table 2 shows the calculated pressure decrease of the vessels with four specified values of pressure and other parameters. The gas consumption rates were calculated backwards from these pressure decrease values, and the results were used in the MELCOR model. Because only four data points were available, the result is a crude approximation of the actual gas consumption rate. The available data was not sufficient for estimating the dependence on temperature or gas species.

Based on the four data points given in (Paladino et al. 2003b) and on the assumption that the gas consumption must approach zero when the pressure approaches zero, the following correlation was derived for the gas consumption  $\dot{V}$  (m<sup>3</sup>/s) as a function of pressure  $p$  (Pa):

$$\dot{V} \approx -5.6 \cdot 10^{-18} p^2 + 1.5 \cdot 10^{-11} p. \quad (1)$$

There are 18 control volumes that have gas sampling lines. The sampling was modeled as 18 time-dependent flow paths from the corresponding volumes to the time-independent environment volume. Each of them draws the volumetric flow rate calculated with equation (1), multiplied by the number of sampling lines in the control volume.

#### 4.1.8 Helium Injection

Paladino et al. (2003b) write that 12.9 g/s of helium was injected for two hours, beginning at “around” 10 000 s. More accurate numbers can be found in the measurement data. The helium injection started at 10 240 s = 2 h 51 min and ended at 17 440 s = 4 h 51 min. The average measured helium injection rate during this 2 h period was 12.78 g/s and average helium temperature was 32 °C. Thus, the measurement data indicates that 92 kg of helium was injected.

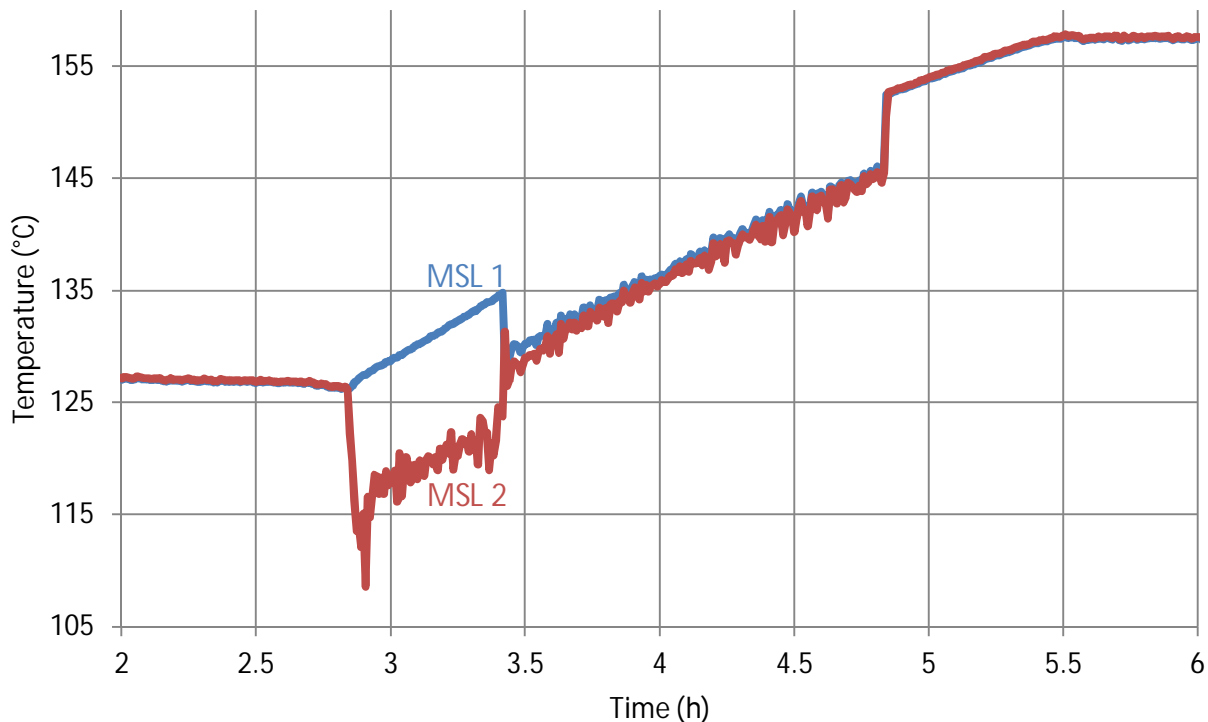
According to the mass spectrometer measurements, practically all the helium has been transported to the wetwells and the GDCS at 5.5 h. The measured partial pressure of helium in the wetwells at this time is 3.5 bar and temperature about 80 °C. Helium density at this pressure is 0.48 kg/m<sup>3</sup>. The wetwell gas volume of 146 m<sup>3</sup> yields 70 kg of helium in the wetwells. The temperature in the GDCS at this time was about 60 °C. Gas concentration in the GDCS was not measured. Assuming the same helium partial pressure in the GDCS as in the wetwells, the helium density there would be 0.51 kg/m<sup>3</sup>. GDCS volume of 18 m<sup>3</sup> yields 9 kg of helium in the GDCS. This is an upper limit because the helium concentration in the GDCS was probably smaller than in the wetwells. Adding these numbers gives a maximum of 79 kg of helium in the facility. If the gas sampling system has decreased the helium partial pressure by 0.1 bar, which is an overestimation, about 2 kg of helium would have been lost. Thus the absolute maximum amount of helium injected to the facility is 81 kg. This is 12 % less than the 92 kg of helium injection that was reported.

Paladino et al. (2003a) present a GOTHIC calculation of the T1.1 experiment. Using the measured injection amount of about 92 kg, they get significantly too high helium concentrations and overestimate the final pressure in the facility by about 1 bar. MELCOR calculation of the experiment with the 92 kg injection, made with the model described in this chapter, gave similar overestimations of both helium concentrations and pressure. Therefore it is concluded that the actual amount of helium injection must have been less than 92 kg.

For the MELCOR model, a best estimate of the amount of injected helium was calculated as follows. 70 kg of helium in the wetwells at 5.5 h is calculated directly from the measurements. But the amount of helium in the GDCS needs to be estimated because gas concentration there was not measured. The MELCOR calculations give about 60 % smaller helium partial pressure in the GDCS than in the wetwells. Thus the amount of helium in the GDCS is estimated to be about 4 kg. The amount of helium lost to the gas sampling system at

5.5 h can be estimated as 1 kg. Thus, the best estimate of injected helium mass is 75 kg. This is 18 % less than the reported 92 kg and 7 % less than the maximum amount of 81 kg.

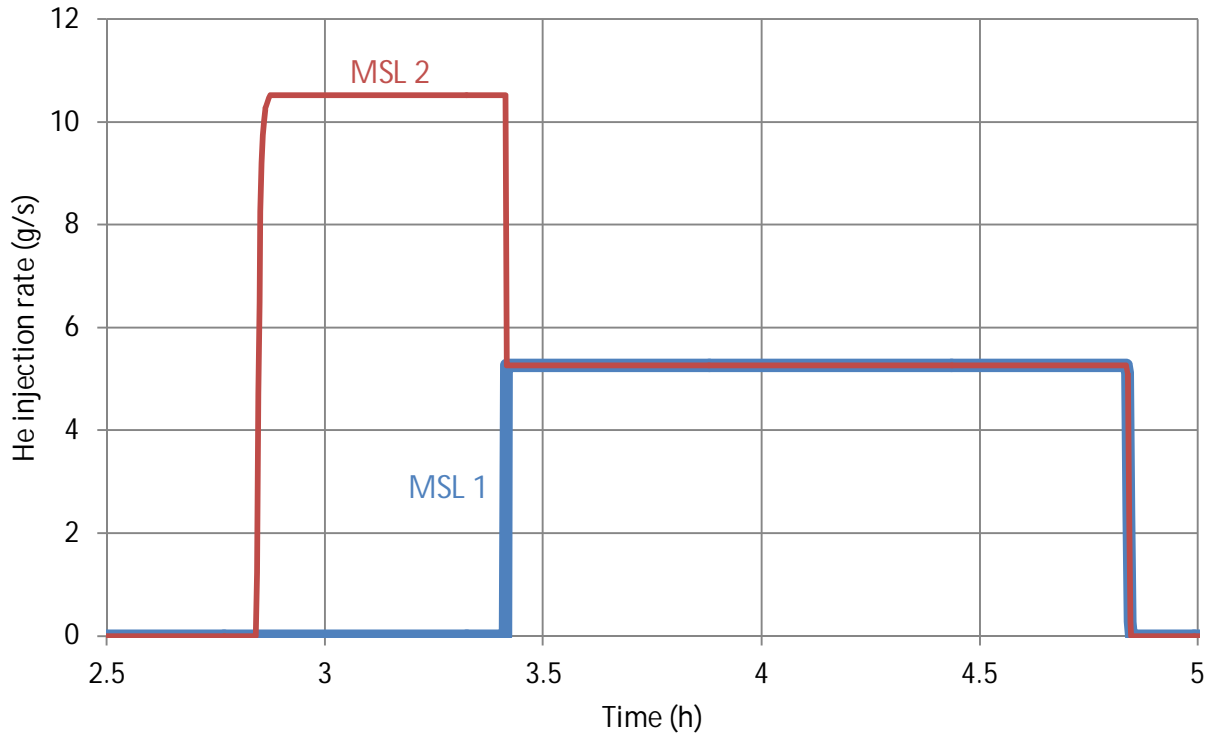
Helium was injected into the main steam lines (MSL). Fig. 23 shows measured temperatures at the exit of both steam lines. Start of helium injection at 2 h 51 min is clearly visible in the MSL 2 curve. However, there is a clear asymmetry for the first 34 min, with MSL 1 temperature significantly higher than MSL 2 temperature. This indicates that more helium was injected into MSL 2 than into MSL 1. At 3 h 25 min the asymmetry disappears.



**Fig. 23.** Measured temperatures at the exit of main steam lines 1 and 2.

The helium source in the MELCOR model was defined as follows. First, the measured injection rate was multiplied by 0.82 to get from the measured 92 kg to the estimated 75 kg. Then the asymmetry between the main steam lines 1 and 2 was accounted for by feeding all the helium to MSL 2 during the first 34 min. After this, equal amounts of helium were injected to both steam lines. The resulting injection rates are shown in Fig. 24. This gave a very good match between the measured and calculated main steam line temperatures. Also the measured helium concentrations were reproduced well, as can be seen in section 4.3.1.3.

Using different helium injection rate in the model than what is given in the experiment report of course requires very good reasoning. Assuming that the helium injection rate measurement is *correct* would have three consequences: 1) The mass spectrometer would underestimate helium concentrations by at least 12 %; 2) The MELCOR model of the facility would be wrong because it would give much too high pressure; and 3) The GOTHIC model of Paladino et al. (2003a) would be wrong because it also gives much too high pressure. It is considered more probable that the helium injection rate measurement is wrong than that the helium concentration measurement and both MELCOR and GOTHIC models would be wrong. This justifies modifying the helium injection rate in the model.



*Fig. 24. Helium injection rates to the main steam lines in the MELCOR model.*

## 4.2 Modeling the PCC Units

### 4.2.1 Nodalization

A drawing of a PCC unit was shown in Fig. 7. MELCOR nodalization of PCC 1 is shown in Fig. 25. The feed line is CV 88. The upper header was divided into upper and lower control volumes, CV 102 and 103. The reason for this division was proper modeling of helium concentration. When there was upwards flow in some of the PCC tubes, calculated helium concentration in the lower part of the inlet plenum was higher than in the upper part. This is explained by the higher density of cold helium rich gas mixture coming up from the PCC tubes than the density of the warmer gas mixture in the upper part of the header.

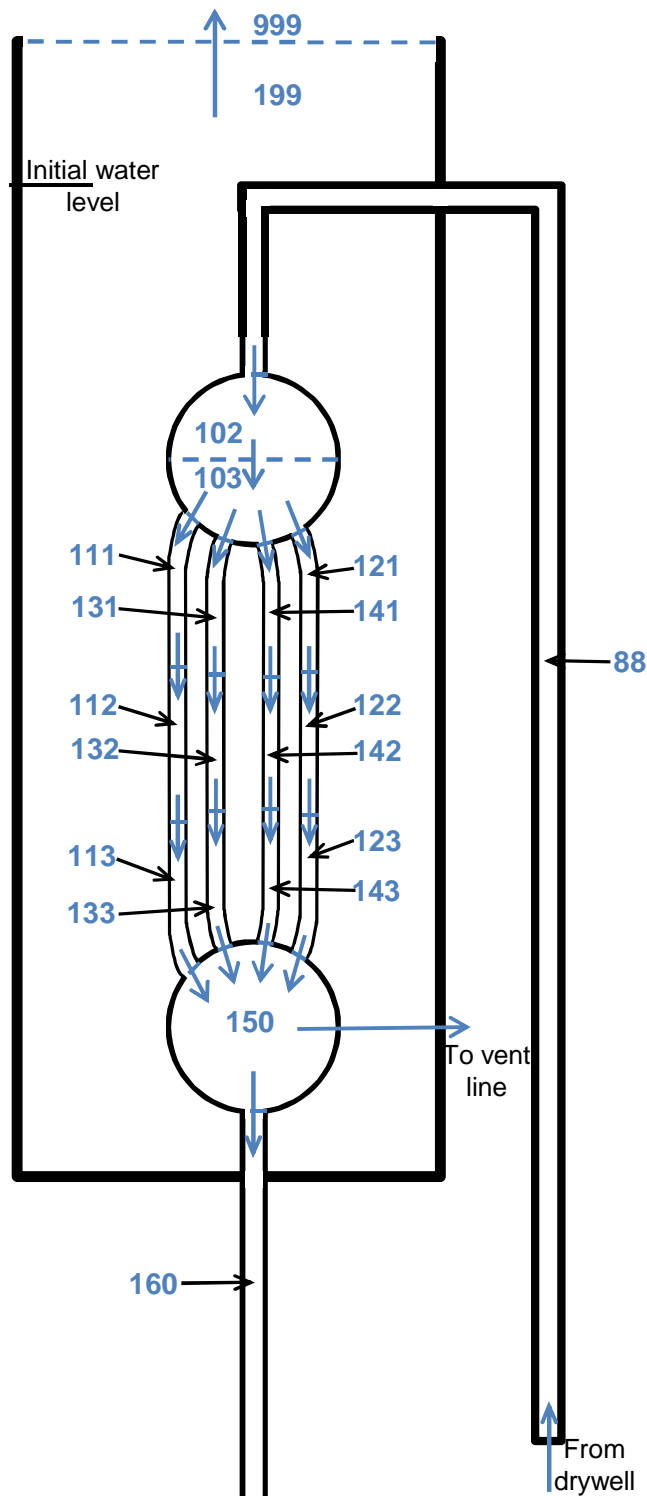
The 20 PCC tubes were divided into 4 groups. Each group represents 5 tubes of equal length. The longest tubes are group 1, CV 111–113. The second longest tubes are group 2, CV 121–123. The third longest tubes are group 3, CV 131–133. The shortest tubes are group 4, CV 141–143. Each tube group was divided into three control volumes of equal lengths in the vertical direction. Each heat structure representing the tube walls had multiplicity of 5 in order to model the 5 identical tubes.

The lower header was modeled as a single control volume 150. The drain line is CV 160. The three drain lines combine into a single line, CV 94, leading to the RPV, see Fig. 18. The intersection is below water level, so that gas cannot flow between lower headers of different PCC units.

The PCC pool was divided into two control volumes, 198 and 199. The PCC heat structures were interfaced to CV 199. CV 198 represents the other half of the pool, but it is not shown in Fig. 25. These adjacent pool volumes were connected with two flow paths at different elevations to allow flow to both directions. Both of the pool volumes were connected to the time-independent environment volume 999. The initial water temperature was about 96 °C. It could be beneficial to divide the pool into several control volumes in the vertical direction



because the saturation temperature is slightly higher in the lower parts due to the hydrostatic pressure. This was not tested.



**Fig. 25.** Nodalization of PCC 1. Control volumes are marked by blue numbers and their borders are drawn with blue dashed lines. The blue arrows are flow paths. The other two PCC units had identical nodalization but different volume numbers.

Lübbesmeyer et al. (1999) does not give information about insulation of the PCC feed line that is submerged in the water pool. However, in (Stempniewicz 2000, section IV.D.2), it is

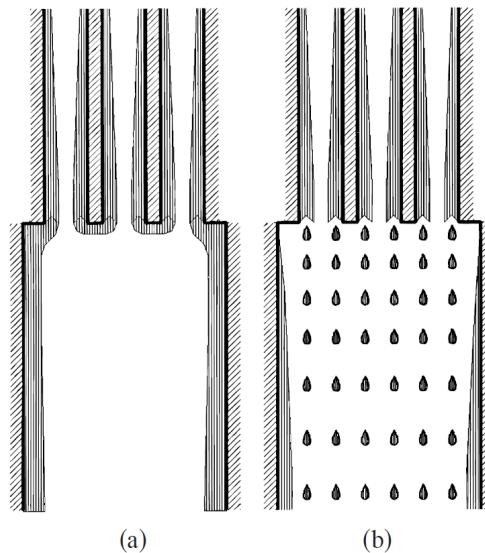
said that the feed line was insulated except for a 15 cm part just above the PCC inlet header. This information was used in the MELCOR model.

#### 4.2.2 Heat Loss from the Pool

Lübbesmeyer et al. (1999) section 3.3 reports a measurement of heat losses from a PCC pool. The water was heated to nearly saturation temperature and the cool-down of the water was measured under non-boiling conditions when there was no load on the primary side of the PCC. The measured heat loss was about 40 kW per pool. This measurement was modeled with MELCOR and the form loss coefficients of the pool flow paths were adjusted so that the measured heat loss was obtained. Walls of the PCC pool were not modeled as heat structures because heat loss through the insulated walls is negligible compared to the heat loss from the pool surface.

#### 4.2.3 Condensate Drainage Modeling

When a smooth vertical structure is modeled as several heat structures, it is obvious that MELCOR's film tracking model has to be used. This properly takes into account the fact that the condensate film is thicker in the lower part of the structure, which decreases the heat transfer rate. But a more difficult issue is treatment of the condensate in places where the structure is not smooth: 1) condensate coming from the feed line to the upper header; 2) condensate coming from the upper header to the tubes; 3) condensate coming from the tubes to the lower header; and 4) condensate coming from the lower header to the drain line. Two options for the behavior of the water in case 3 is illustrated in Fig. 26. Stempniewicz (2000) concludes that option (b) is physically correct. The water flows down as droplets instead of forming a film on the walls of the lower header. There may be some condensation on the surface of the droplets, but this effect is small because the droplets are close to saturation.



**Fig. 26.** Condensate flow from the PCC tubes to the lower header. (Stempniewicz 2000)

It was found out that treatment of the drainage of the condensed water inside the PCC unit is very important for the numerical stability of the calculation. If a film tracking network is defined only for the structures that form a smooth vertical structure, water pools are formed at the bottom of each control volume. Water condensed in the upper header would form a pool in CV 103. This water would flow to the tubes and form a tiny levitating pool in CV 141, 142 and 143. There would also be a pool in CV 150, even though the water level in the drain line,

CV 160, is significantly below the bottom elevation of CV 150. These levitating pools caused serious oscillation and very short time steps in the MELCOR calculation.

The problem of levitating pools was solved by defining a small auxiliary heat structure that was interfaced to the drain line, CV 160. MELCOR's film tracking model was used for guiding the drainage directly to this auxiliary heat structure from the following structures: PCC feed line (the part that is interfaced to the pool), lower part of the upper header, lowest parts of the PCC tubes, and the lower header. From the auxiliary structure the water drained to the pool of CV 160. As a result, the condensed water "jumped" directly to the drain line instead of forming tiny levitating pools at the bottom of each control volume. Avoiding the levitating pools also required activation of the Radionuclide (RN) package for modeling settling of fog from upper to lower control volumes. Otherwise the fog would have formed levitating pools. Activation of the RN package slowed down the calculation about six-fold.

Another possibility for solving the problem of levitating pools, and the oscillation caused by them, would be the spray model. Condensed water could be transferred to the Spray package, which would transfer the droplets through several control volumes without forming pools. This approach was not tested. The spray modeling would require four spray trains passing through the lower header, one from each tube group, but MELCOR Users' Guide warns that multiple spray trains in one control volume can cause non-physical results.

## 4.3 Results

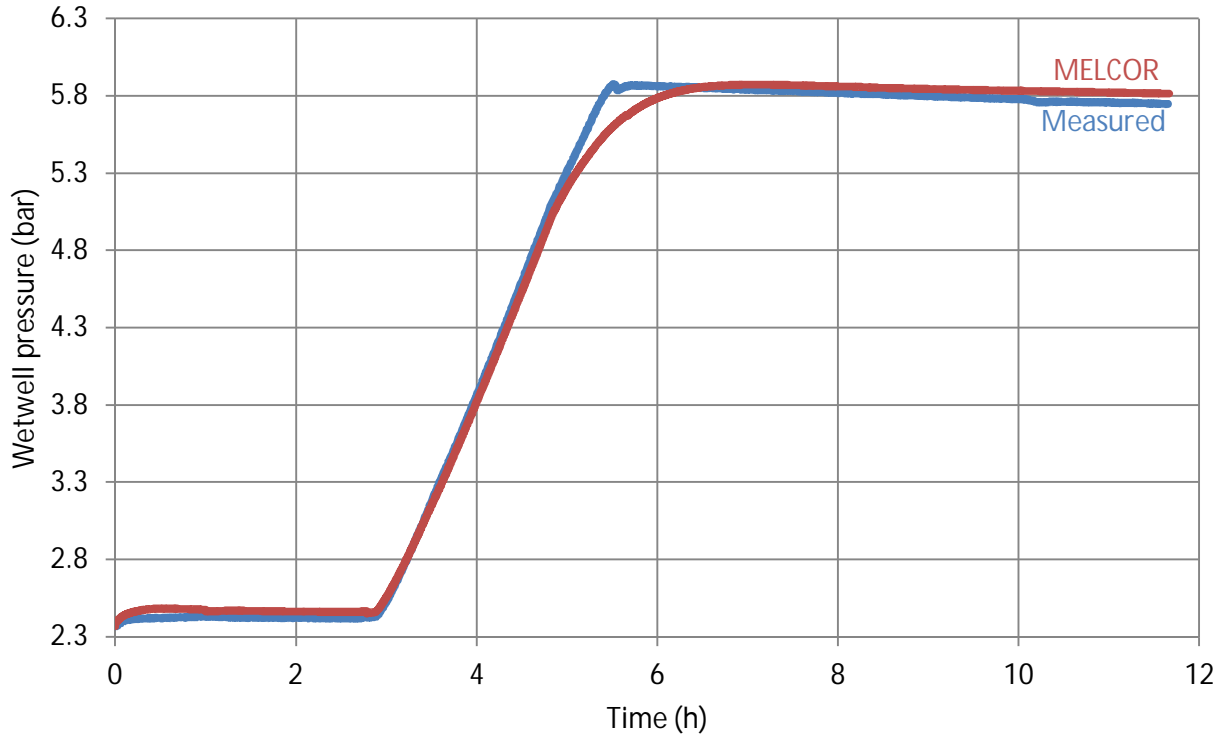
The calculations were made with MELCOR 2.1 revision 3226. The maximum time step was set to 0.02 s. The calculation took 39 h of cpu time with Intel Core i5 M540. It was 3.4 times slower than real time. Results of the base case calculation of the PANDA T1.1 experiment are reported in section 4.3.1. A simplified PCC nodalization was tested, and its results are given in section 4.3.2. In order to get more insights to the PCC behavior, the experiment was calculated with the heating power increased by 10 % from the actual. This case is reported in section 4.3.3.

### 4.3.1 Base Case

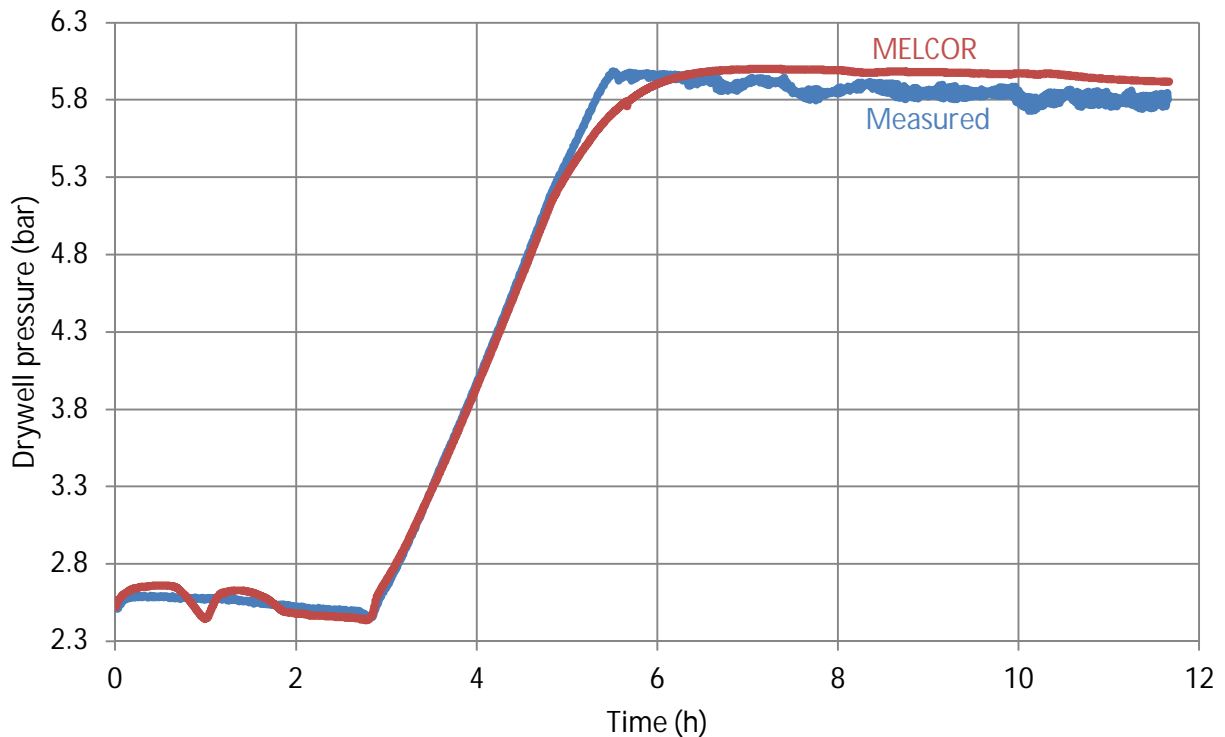
#### 4.3.1.1 Pressures and Flow Rates

The wetwell pressure is shown in Fig. 27. The calculation matches very well with the measurement. Only slight underestimation is seen between 5 and 6 h, just after the end of helium injection. The wetwell pressure is overestimated by 0.07 bar at the end of the experiment.

The drywell pressure is plotted in Fig. 28. At 1 h there is a dip in the calculated drywell pressure. The underestimation reaches 0.13 bar, and the vacuum breaker 1 valve briefly opens. 0.13 kg of steam and 1.25 kg of air flows from wetwell 1 to drywell 1, and this restores the pressure to the correct level. Reason for the pressure dip in the calculation was not found. This vacuum breaker opening did not occur in the experiment. Another spurious vacuum breaker opening is calculated at 2 h 47 min, i.e. 4 min before the start of helium injection. This time 0.15 kg of steam and 1.44 kg of air flows to the drywell. In the experiment the vacuum breaker opened at 7 h 46 min and at 10 h 9 min, but these fluctuations did not happen in the calculation. The drywell pressure at the end of the experiment is overestimated by 0.11 bar.



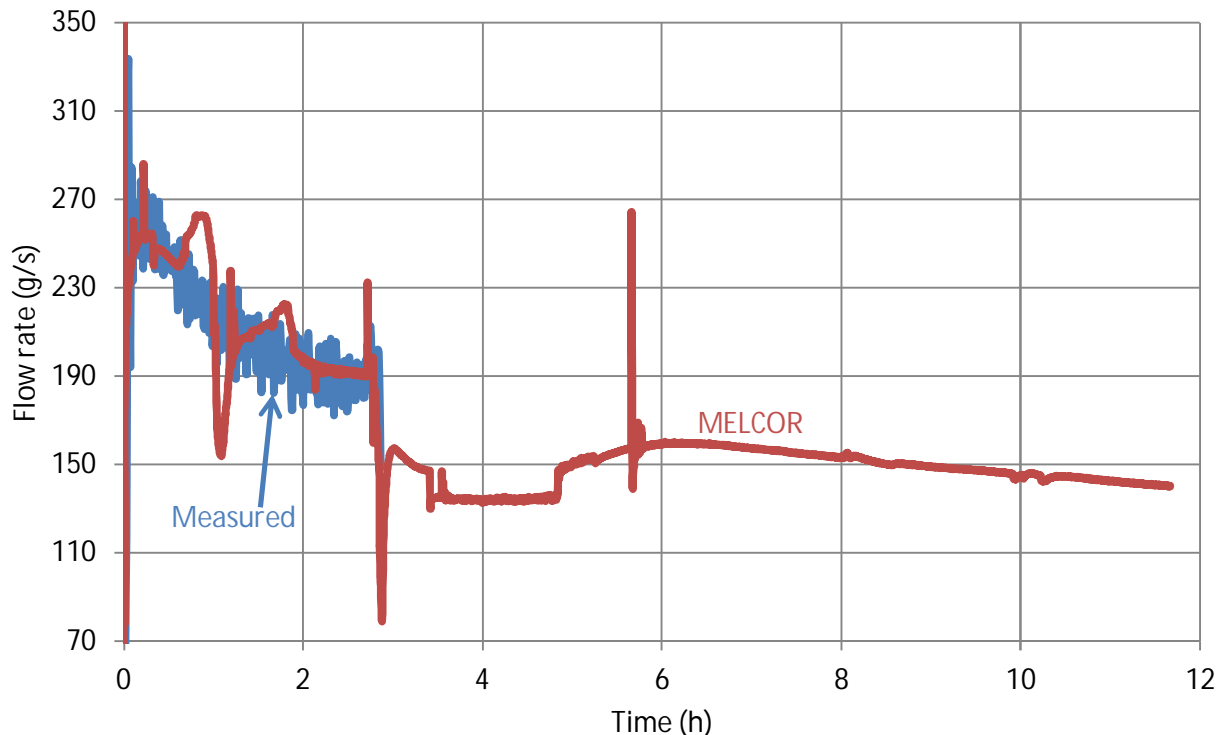
**Fig. 27.** Pressure in the wetwell.



**Fig. 28.** Pressure in the drywell.

The flow rate from the RPV to main steam line 1 is plotted in Fig. 29. Steam line 2 flow rate is almost identical. The flow rate decreases over time because the heating power decreases (Fig. 19). The dip in the calculated pressure at 1 h (Fig. 28) is visible as an increase in the calculated steam flow rate because decreasing pressure causes flashing of water into steam in the RPV. Similarly the calculated pressure increase due to the vacuum breaker opening causes a decrease of the steam flow because the pressure increase causes an increase of the saturation

temperature. Some of the heating power goes into heating the water to the higher saturation temperature, and less power is available for vaporization. For the same reason the steam flow rate is smaller during the helium injection, 2 h 51 min – 4 h 51 min, because the pressure is increasing.



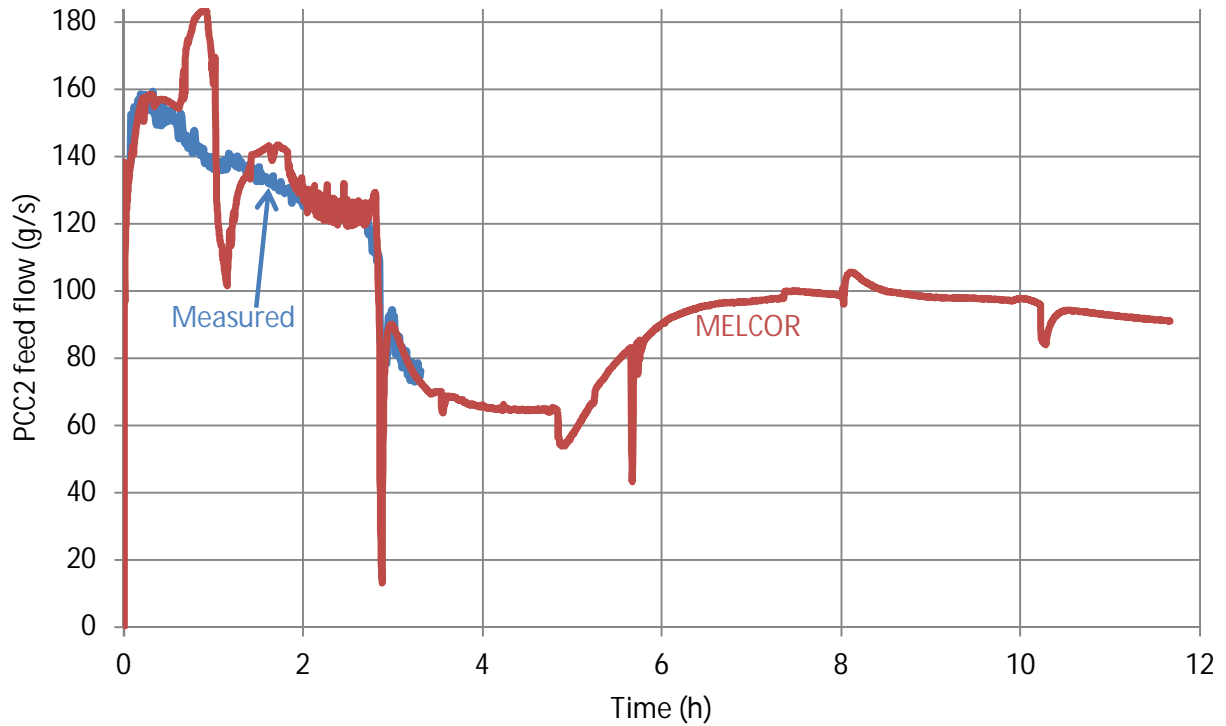
**Fig. 29.** Flow rate from the RPV to main steam line 1. The measured data ends at 2 h 52 min because the flow rate became smaller than the calibration range of the flow meter.

Flow rate in the PCC2 feed line is plotted in Fig. 30. PCC1 and PCC3 had very similar feed flows. The calculated curve looks similar to the main steam line flow rate (Fig. 29). The general level is correct, but the pressure fluctuation at 1 h causes first an overestimation and then an underestimation of the feed flow.

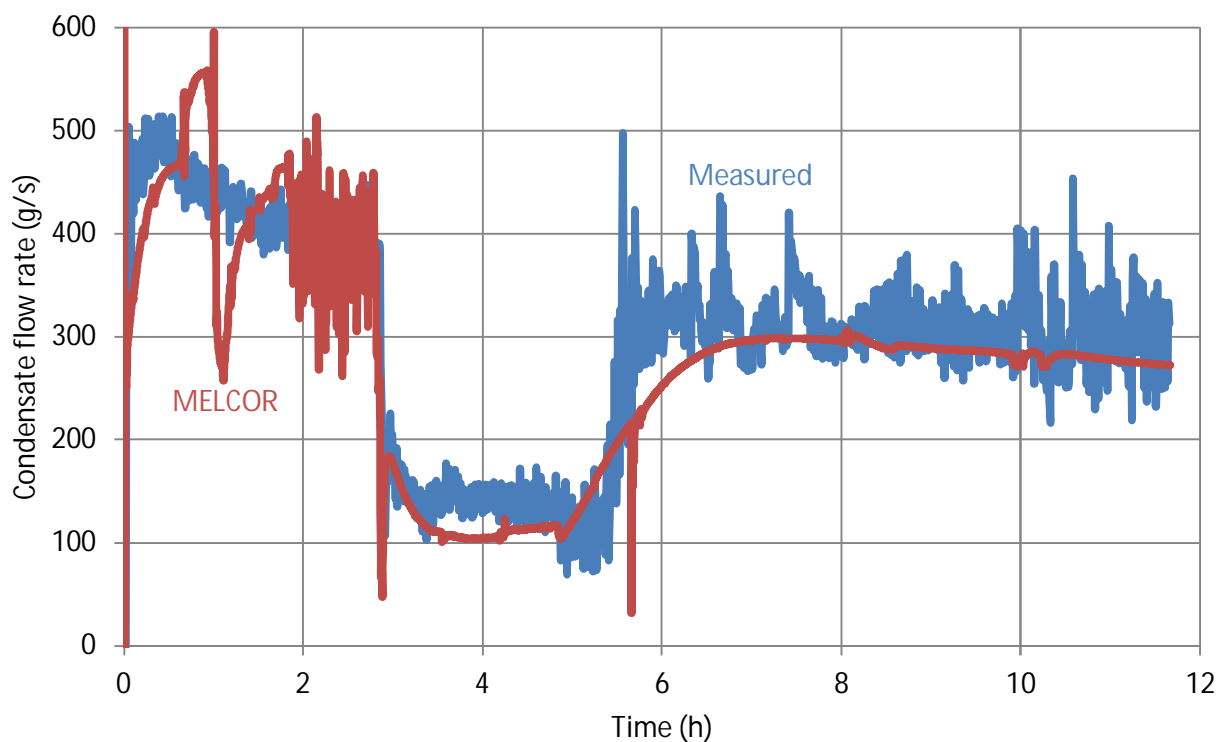
The condensate flow rate from all three PCC units is shown in Fig. 31. At 1 h there is a fluctuation related to the pressure decrease and vacuum breaker opening. After 2 h the calculated condensation rate is oscillating but on the average it is on the same level as the measurement. Helium decreases the condensation rate of the PCCs by about 60 %. The condensation rate is underestimated from the start of the helium injection until the end of the test.

The difference between the measured and calculated condensation in the PCC units is more clearly visible from the integral condensation that is shown in Fig. 32. Until the start of the helium injection at 2 h 51 min, the calculation is very good, with only 2 % underestimation. At the end of the experiment, the underestimation has increased to 7 %.

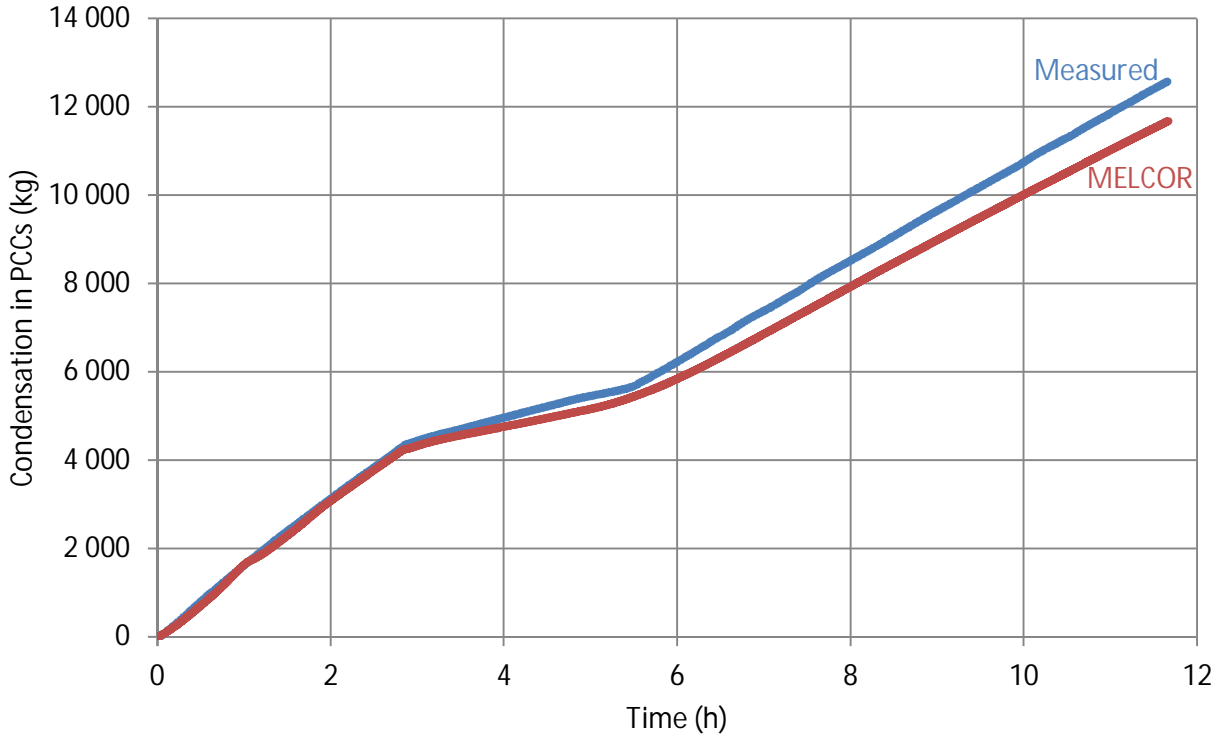
An estimate of the measurement uncertainties can be obtained by comparing the measured condensate mass with the measured integral PCC feed flow. The feed flow rate of all PCC units is in the calibration range of the flow meters until 2 h 51 min. At this time the measured integral condensate flow is 6 % greater than the measured integral PCC feed flow. This would violate mass conservation, so the measurement uncertainties are clearly several per cents. In this view, the 7 % underestimation in the MELCOR calculation is small. However, a similar deviation between the measurement and calculation can be seen in the water levels of the PCC pools (Fig. 33), so the calculation certainly underestimates the condensation slightly.



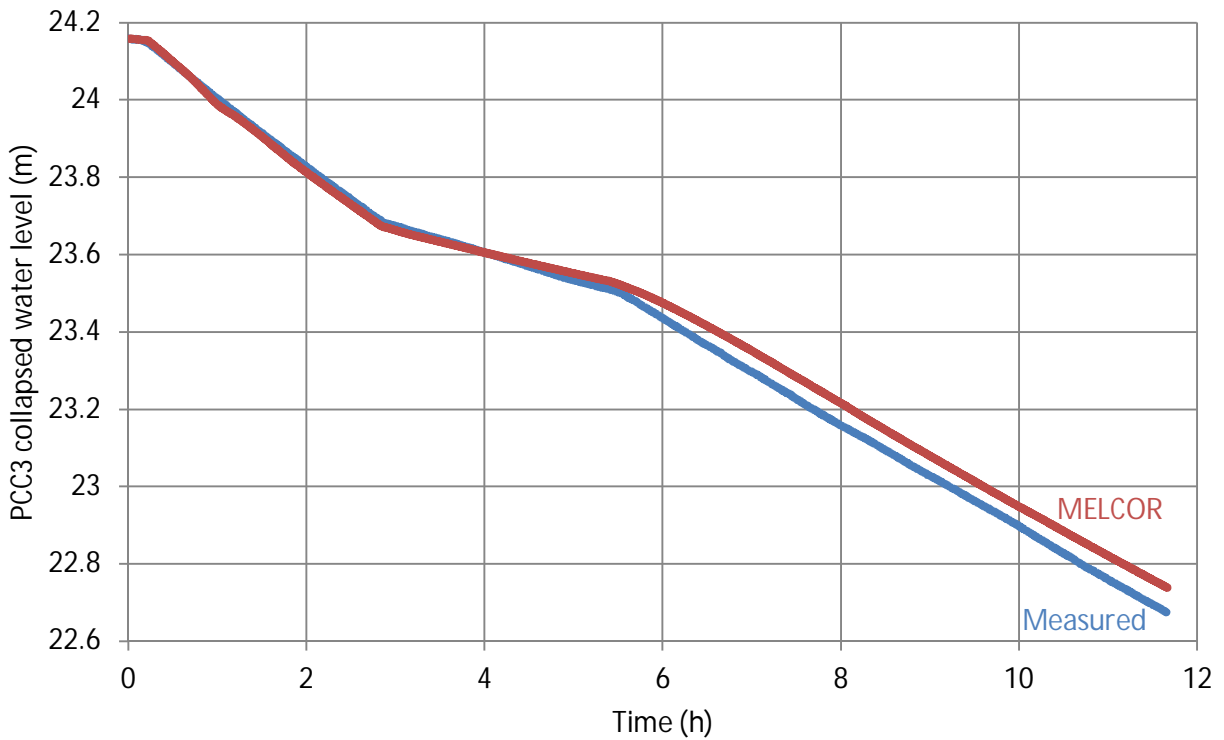
**Fig. 30.** Flow rate in the PCC2 feed line. The measured data ends at 3 h 19 min because the flow rate became smaller than the calibration range of the flow meter.



**Fig. 31.** PCC condensate flow rate, sum of three PCC units.



**Fig. 32.** Integral condensation, sum of three PCC units.



**Fig. 33.** Collapsed water level in PCC3 pool.

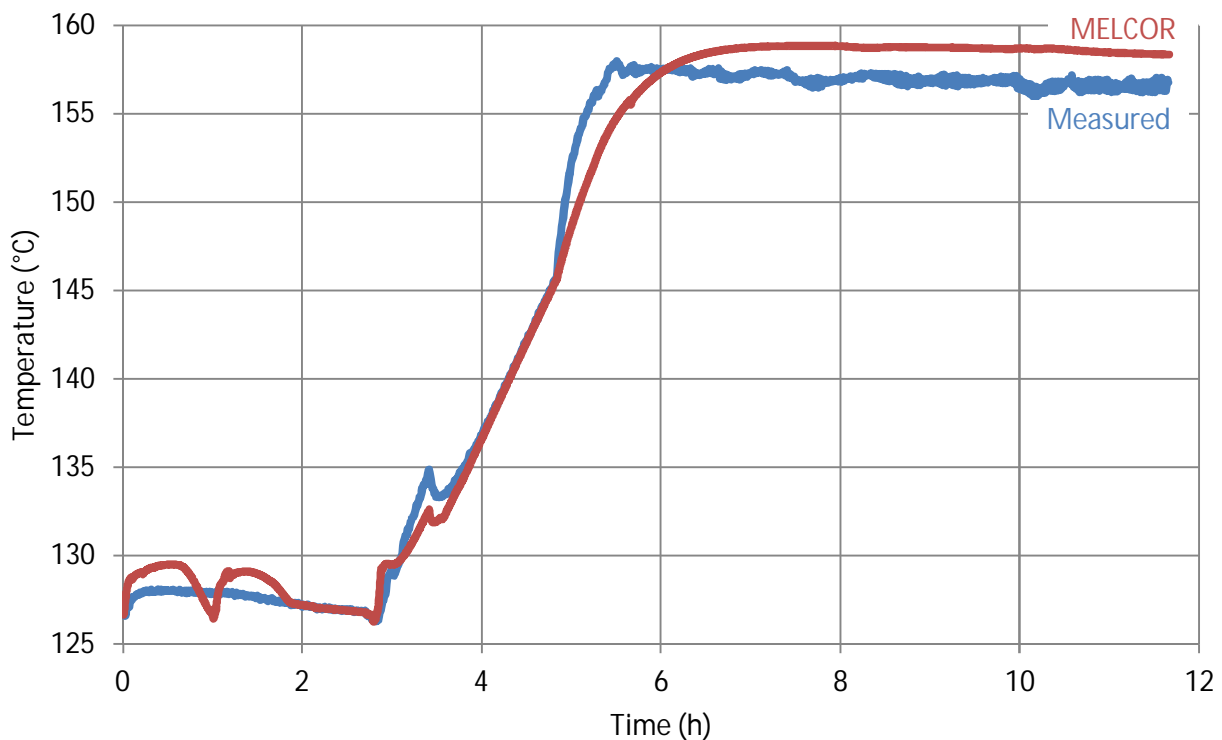
The gas sampling system of the mass spectrometer consumed 13.7 kg of steam, 2.7 kg of air and 0.6 kg of helium. The calculation was made also with the gas sampling system switched off. In this case the pressure at the end of the experiment was 0.04 bar higher both in the wetwell and in the drywell. Thus, the gas consumption of the mass spectrometer had a negligible effect on the calculated pressure. The gas sampling model, presented in section

4.1.7, was based on very limited information. It is possible that the model underestimates the gas consumption of the sampling system.

The base case calculation was made with the modified film Reynolds number limits, as described in chapter 1. When the calculation was repeated with MELCOR's default Reynolds number limits, the total amount of condensed steam in the PCCs became 0.2 % smaller than in the base case. The pressure at the end of the experiment was 0.02 bar higher when the default limits were used. Thus, using the modified film Reynolds number limits improved the results only with a negligible amount.

#### 4.3.1.2 Temperatures

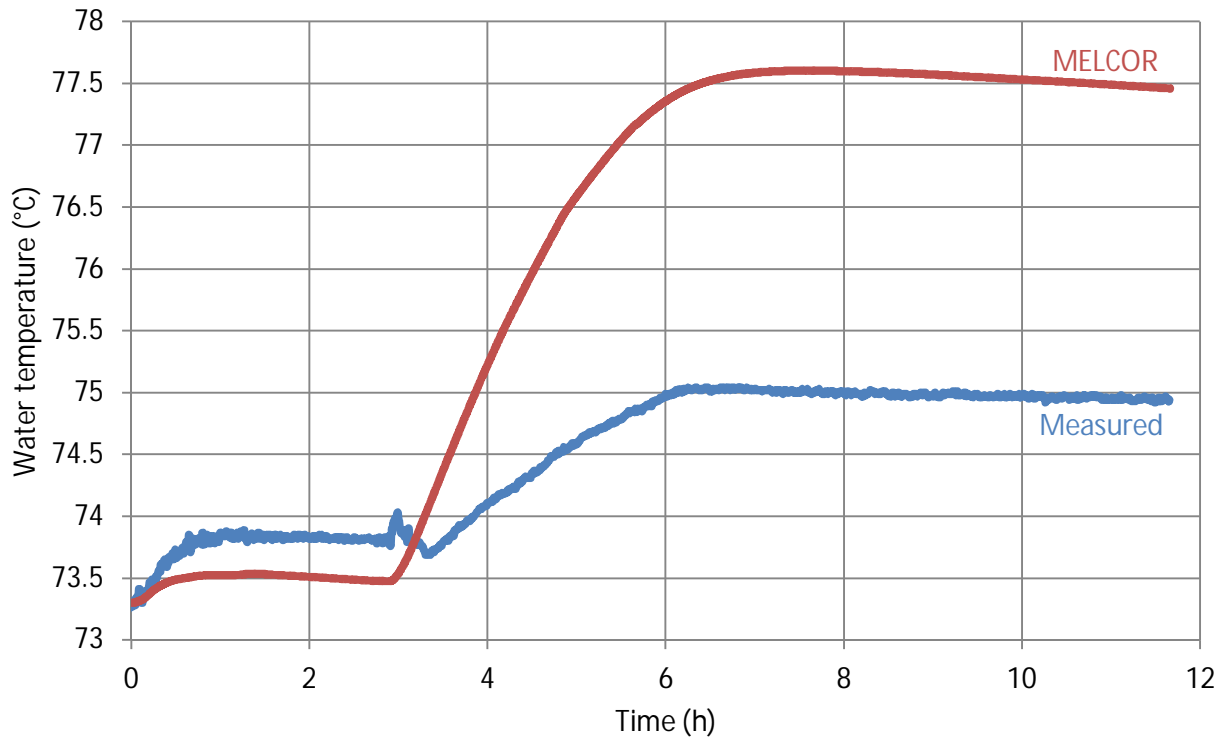
An example of gas temperature in drywell 1 is shown in Fig. 34. The behavior is very similar to the drywell pressure (Fig. 28). The pressure dip and vacuum breaker opening cause fluctuation at 1 h in the calculation, but it did not occur in the experiment. Between 5 and 6 h the temperature and the pressure are slightly underestimated. At the end of the experiment both are slightly overestimated. The other thermocouples in the drywell exhibit a similar behavior. Some temperature stratification was measured between 5 and 6 h, with lower temperatures at the top, but the calculated temperatures remained uniform.



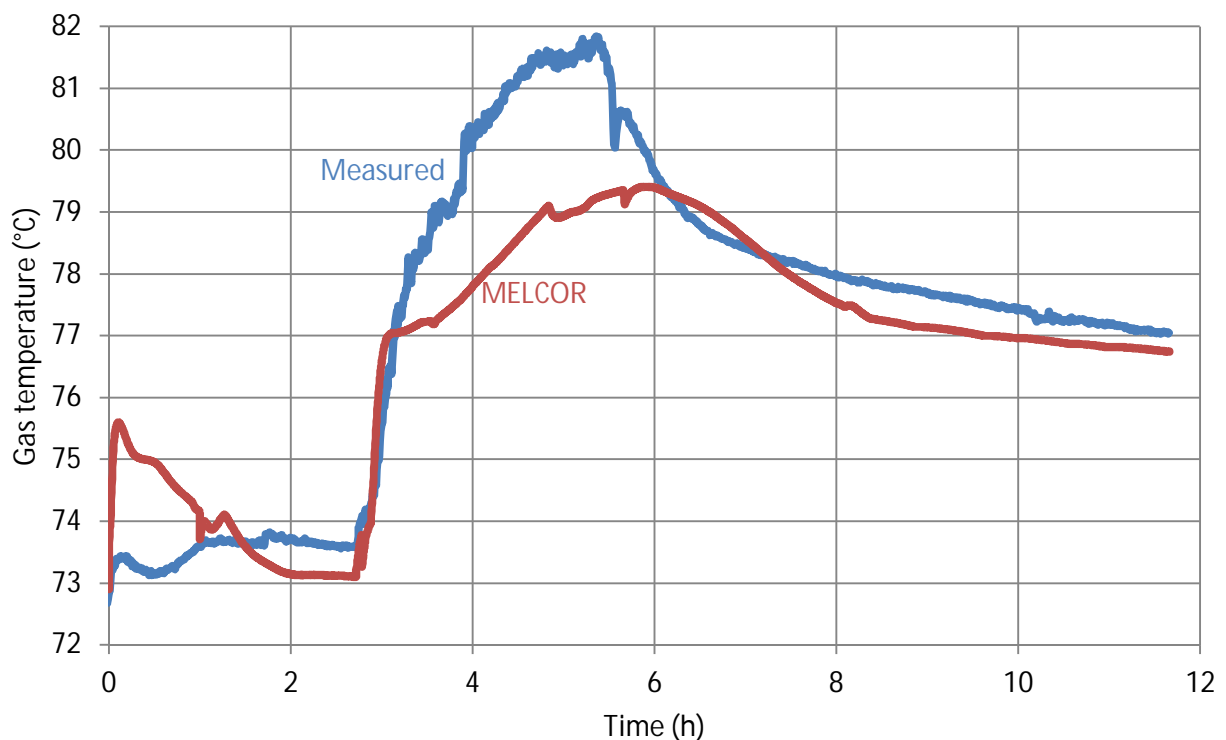
**Fig. 34.** Temperature in drywell 1 (CV 13 in the MELCOR model, thermocouple MTG.DIC.10 in the experiment).

Water temperature in wetwell 1 is plotted in Fig. 35. The plot is from CV 42, but the bottom volume, CV 41, had almost identical calculated water temperature after 10 min. Before helium injection the temperature is slightly underestimated, by 0.3 °C. This happens because MELCOR calculates too much mixing with the bottom volume, CV 41, while in the experiment the bottom of the pool, which is not shown in the plot, was slightly cooler. After the helium injection the calculated temperature is 2.5 °C higher than the measured. Probably the temperature of the helium coming from the PCC vent line was overestimated, and this heated up the water. An example of gas temperatures in the wetwell is plotted in Fig. 36. The match is quite good.





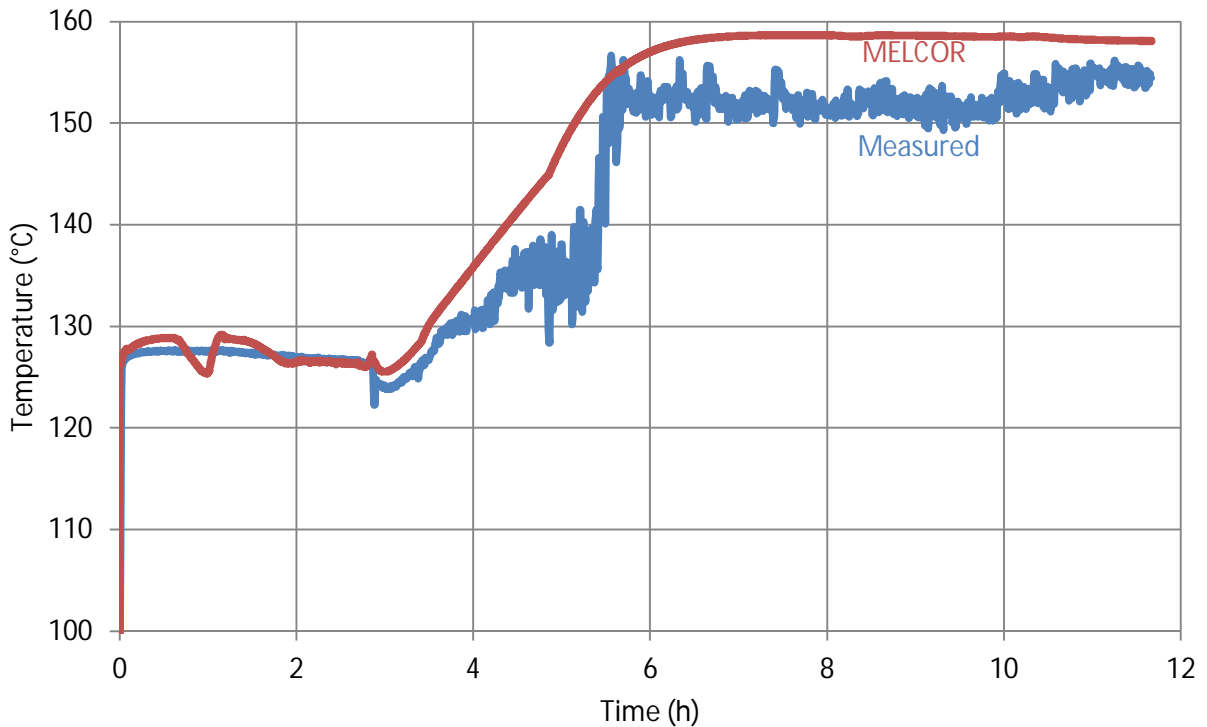
**Fig. 35.** Water temperature in wetwell 1 (CV 42 in the MELCOR model, average of thermocouples MTL.S1.1–MTL.S1.5 in the experiment).



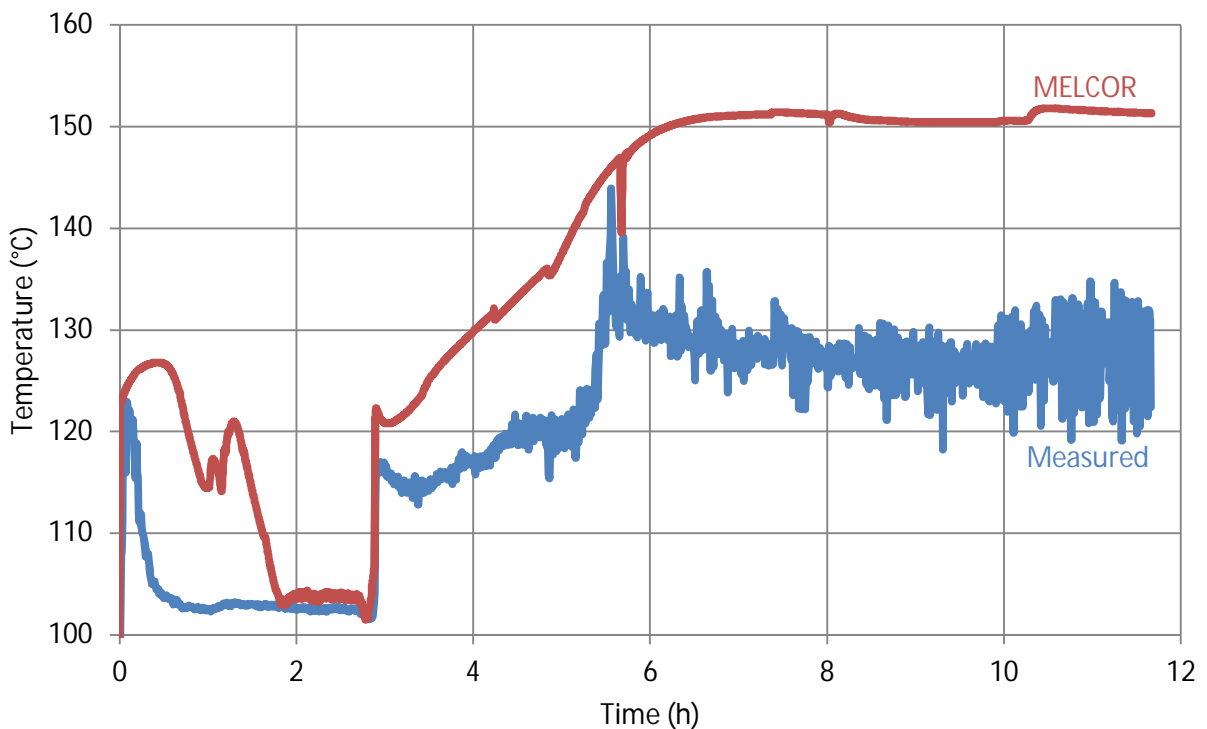
**Fig. 36.** Gas temperature in wetwell 1 (CV 44 in the MELCOR model, average of thermocouples MTG.S1.2–MTG.S1.4 in the experiment).

Gas temperatures in PCC2 upper and lower header are shown in Fig. 37 and Fig. 38. The other two PCC units have similar temperatures. The upper header temperature is calculated quite well, with a few degrees overestimation after the start of the helium injection. The lower header temperature is significantly overestimated for most of the time. Only around 2 h there

is a 1 h period when the calculated temperature is correct. At the end of the experiment the overestimation is more than 20 °C. The calculated temperature follows the saturation temperature at the partial pressure of steam in the lower header. Thus, the steam partial pressure in the lower header is probably overestimated and the concentration of non-condensable gases is underestimated.



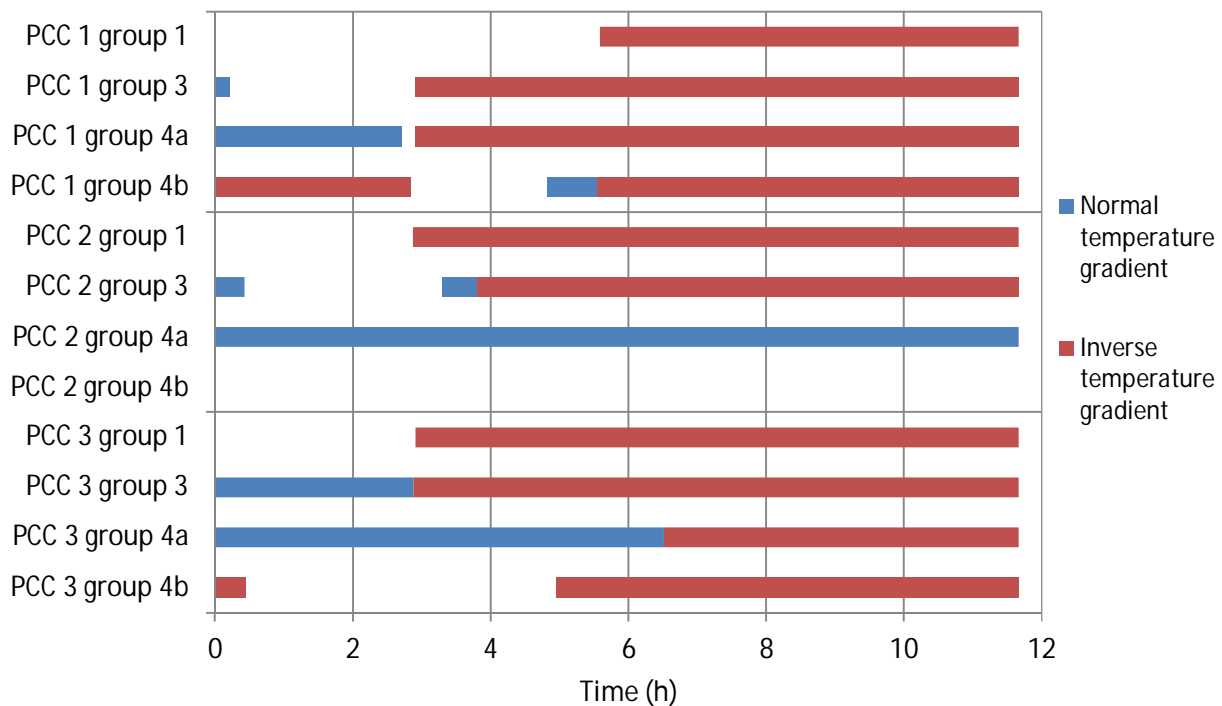
**Fig. 37.** Temperature in PCC2 upper header (CV 202 in the MELCOR model, thermocouple MTG.P2.1 in the experiment).



**Fig. 38.** Temperature in PCC2 lower header (CV 250 in the MELCOR model, thermocouple MTG.P2.2 in the experiment).

When the flow direction in a PCC tube is downwards, one would expect that the top of the tube is hotter than the bottom. In the following discussion this case is called *normal temperature gradient*. In some cases the measurement data of both gas temperatures and tube wall temperature show the opposite: the top of the tube is cooler than the bottom. This is called *inverse temperature gradient*. It is thought that an inverse gradient means that the flow direction is upwards (Paladino et al. 2003b), but this interpretation is uncertain.

Fig. 39 shows measured temperature gradients in the experiment. Four tubes in each PCC unit had thermocouples inside the tube walls. One of the four tubes had thermocouples also inside the tubes, measuring the gas temperature. The figure is based on both wall and gas temperature measurements. The longest tubes are called group 1 and the shortest tubes are called group 4, just like in the MELCOR model description in section 4.2.1. There were no thermocouples in the second longest tube group. Two tubes in group 4 were instrumented, 4a and 4b. There are periods when the direction of the temperature gradient is not clear. They are left as white areas in the figure. PCC 2 group 4b is unclear because the middle of the tube was hotter than the top and bottom throughout the test.



**Fig. 39.** Measured temperature gradients in PCC tubes. Normal gradient, blue bar, means that top of tube is hotter than bottom. Inverse gradient, red bar, means the opposite. White areas are time periods when the gradient could not be unambiguously determined. The longest PCC tubes are group 1, and shortest tubes are group 4.

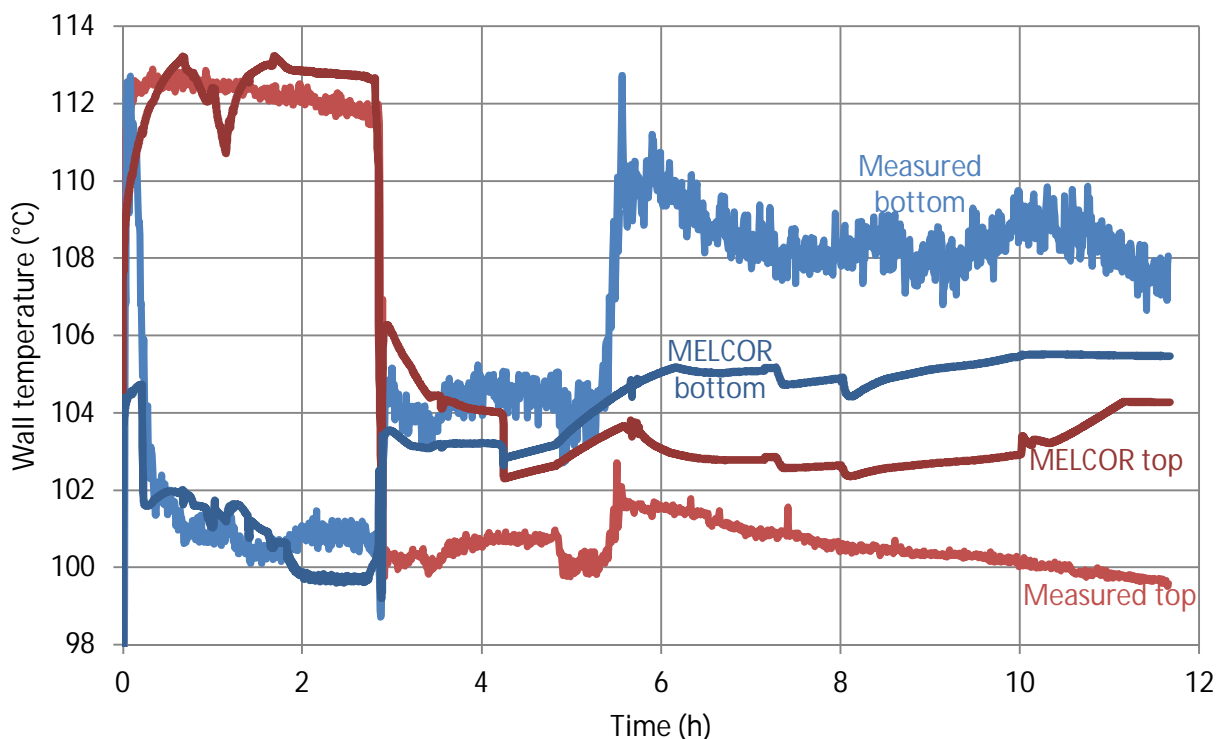
One would expect that in the beginning of the test, before helium injection, all the tubes would have downwards flow and normal temperature gradient. When helium enters the PCC, the flow can change direction in some of the tubes due to the buoyancy of helium. But the results are surprising.

In the very beginning of the experiment, group 4b tubes in PCC 1 and 3 have an inverse temperature profile. When helium is injected at 2 h 51 min, almost all the instrumented tubes change to inverse temperature gradient. At the end of the test, only one of the tubes has normal gradient. There are two possible interpretations for this. First, it could be possible that the effect is real and, by coincidence, all the ten tubes really did have upwards flow. There are 48 tubes that did not have thermocouples, and the gas can be flowing downwards in these

tubes. The second possible interpretation is that the inverse temperature gradient might not necessarily mean that the flow direction is upwards. No dependence on tube length can be seen in the measured temperature gradients.

In the MELCOR calculation, all tubes have downwards flow until 4 h 11 min. At that time the flow in the longest tubes, group 1, reverses its direction almost simultaneously in all three PCC units. The flow reversal changes the calculated temperature gradient from normal to inverse. All other tube groups remain in downwards flow and normal temperature gradient.

As an example of the PCC tube temperatures, Fig. 40 shows the measured and calculated temperatures of tube walls in PCC 3 tube group 1, i.e. the longest tubes. The thermocouples were inside the tube wall, so they measured the wall material temperature instead of surface temperatures. Similarly, the MELCOR results were taken from node 2, which was at the center of the tube wall. (The heat structures had 3 nodes.)



**Fig. 40.** Wall temperatures of PCC 3 longest tubes (center node of heat structures interfaced to CV 311 and 313 in the MELCOR model, thermocouples MTT.P3.11 and MTT.P3.13 in the experiment).

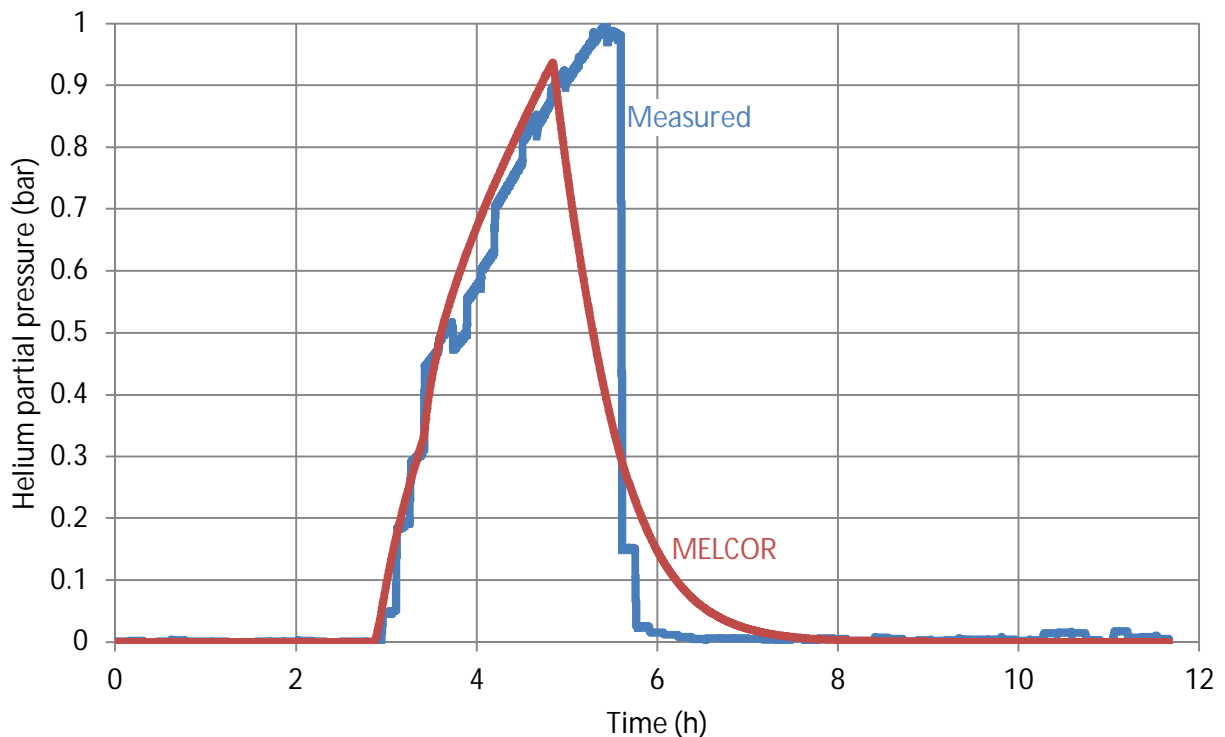
Fig. 40 shows that until the start of helium injection at 2 h 51 min, the match between the measurement and calculation is very good. The top of the tube is about 11 °C hotter than the bottom part. In Fig. 39 this period is classified as an unclear temperature gradient and colored white because the thermocouple in the middle of the tube, which is not shown in Fig. 40, measured a higher temperature than that at the top of tube.

When helium enters the PCC, the temperatures change drastically. The top of the tube drops to 100 °C, while the bottom of the tubes heats up to 104 °C. An inverse temperature gradient occurs. At 5.5 h the helium concentration decreases and the tube bottom temperature rises by several degrees due to the increased heat transfer rate. However, the top of the tube remains cool and the temperature gradient is inverse, which might indicate upwards flow. In the MELCOR calculation the flow reversal occurs at 4 h 15 min, and it causes an inverse temperature gradient. However, the difference between the top and bottom temperatures

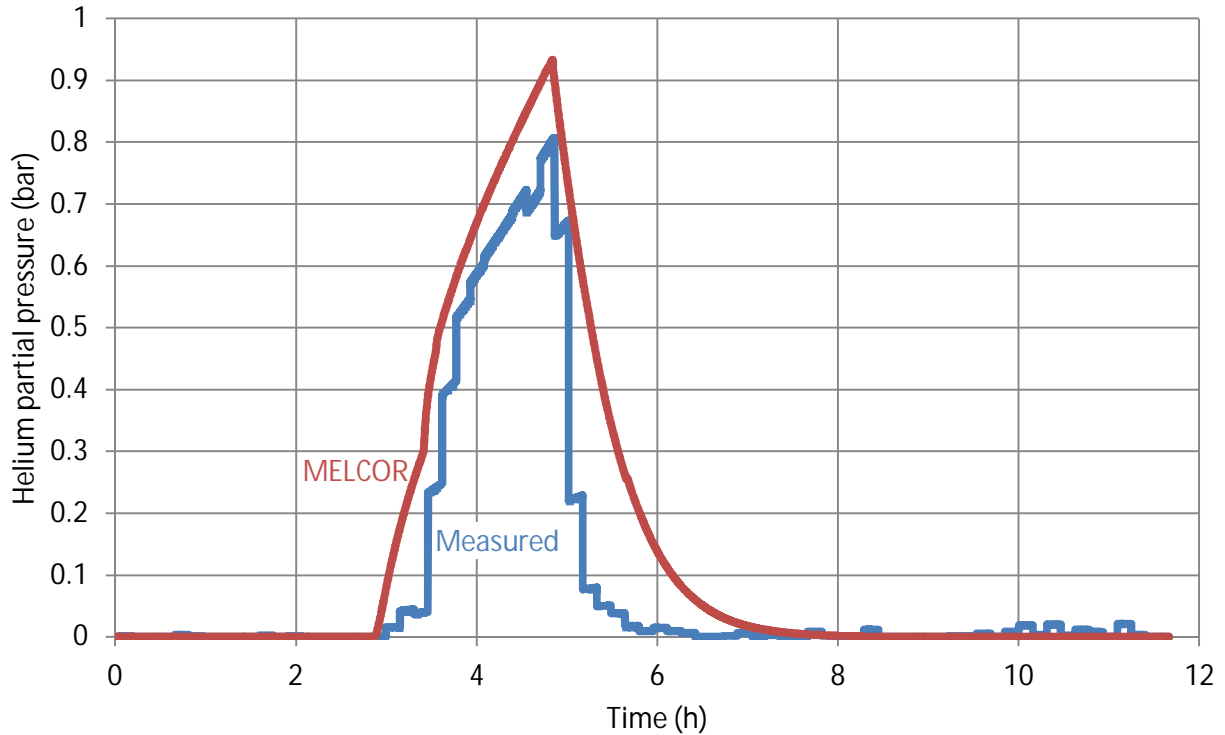
remains much smaller in the calculation than in the measurement. Flow fields in the condenser have also been investigated with the CFD code Fluent by Tuomainen (2003).

#### 4.3.1.3 Helium Concentrations

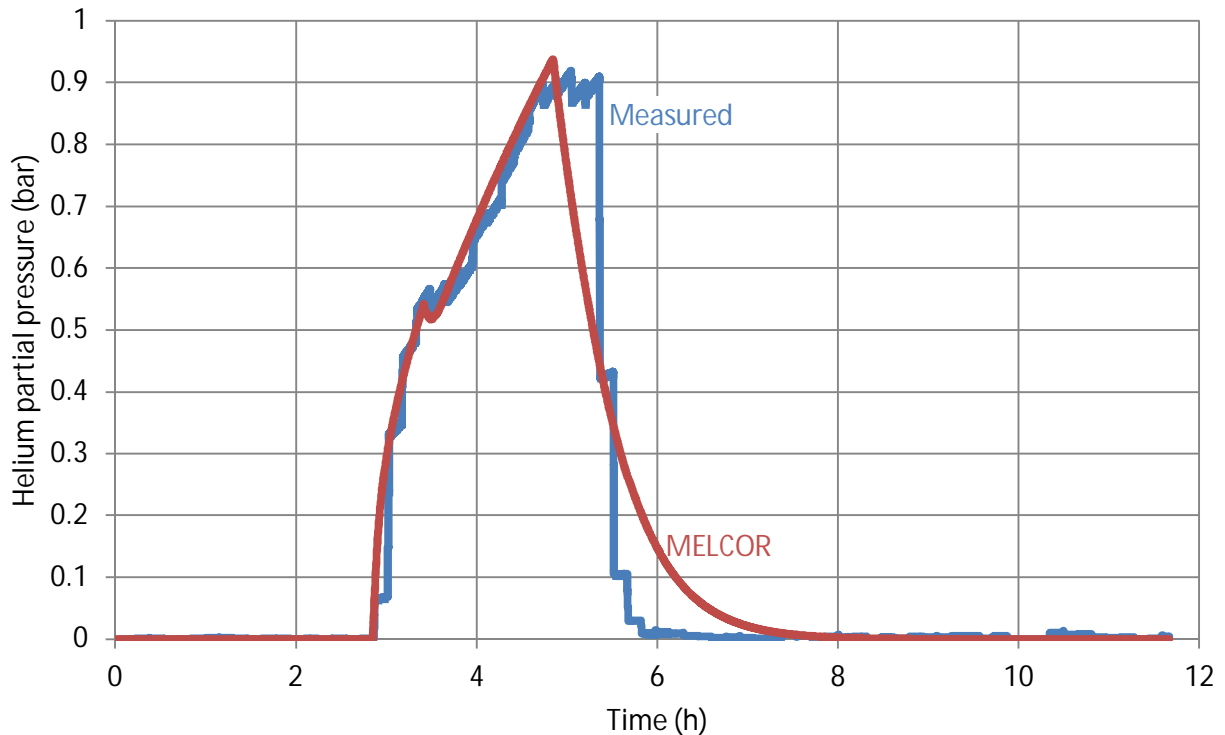
Partial pressure of helium in three locations in the drywells is presented in Fig. 41, Fig. 42 and Fig. 43. The increasing helium concentration during the helium injection is calculated quite well at the top of the drywells (Fig. 41 and Fig. 43). Some stratification occurred in the experiment, because the helium concentration at the lower parts of the drywell (Fig. 42) was smaller than at the top. The MELCOR model fails to calculate this stratification. The calculated helium concentration is uniform at all elevations. MELCOR underestimates the helium outflow rate from the drywells. The helium concentration in the drywells is therefore overestimated after 5 h 40 min.



**Fig. 41.** Partial pressure of helium at the top of drywell 1 (CV 16 in the MELCOR model, average of gas sampling ports D1A.1, D1B.1 and D1C.1 in the experiment).



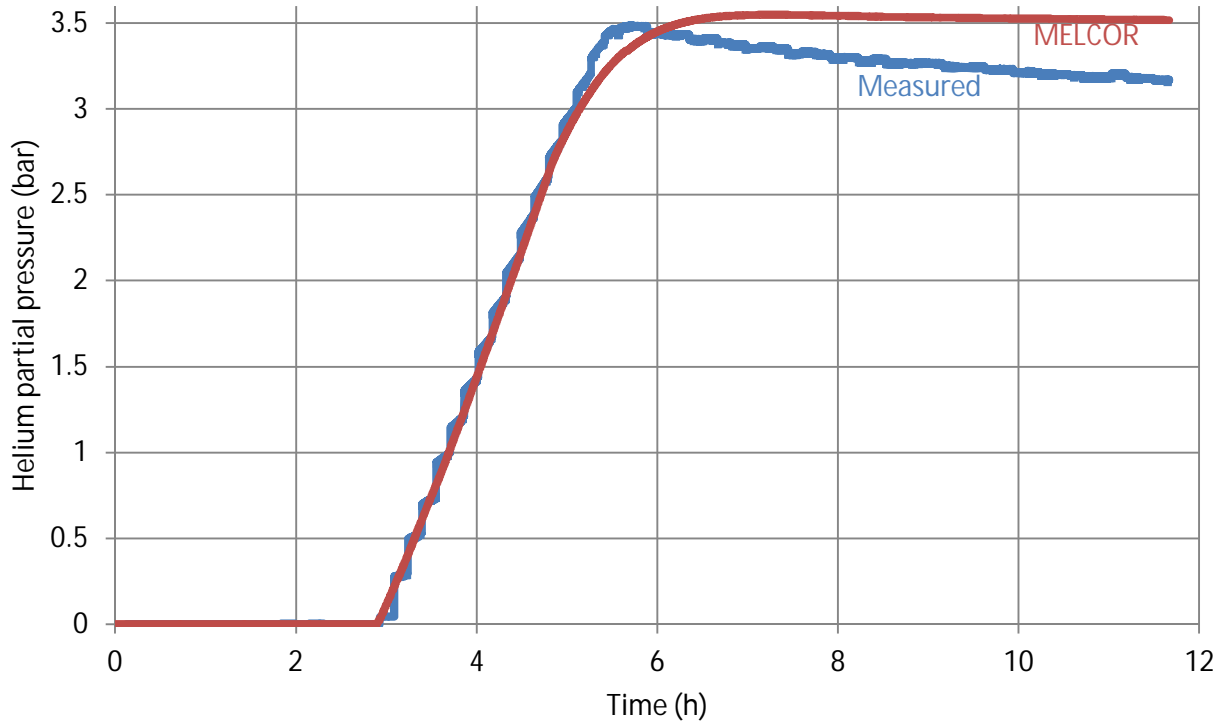
**Fig. 42.** Partial pressure of helium in CV 13 in drywell 1 (gas sampling port DIC.3).



**Fig. 43.** Partial pressure of helium at the top of drywell 2 (CV 26 in the MELCOR model, average of gas sampling ports D2A.1, D2B.1 and D2C.1 in the experiment).

The helium concentration in the wetwells was uniform both in the calculation and in the measurements. The partial pressure of helium at the top of wetwell 2 is shown in Fig. 44. During the helium injection period, until 4 h 51 min, the match between the calculation and the measurement is very good. The abovementioned underestimation of helium outflow rate from the drywells is visible as a short-term underestimation of the helium concentration in the

wetwell before 6 h. The peak helium concentration in the wetwell is slightly overestimated. This confirms that using the smaller amount of helium injection in the MELCOR model than what was indicated in the test report was appropriate (section 4.1.8). The measured helium concentration in the wetwell decreases in the end of the experiment probably because helium flows to the GDCS tank. The calculation shows a smaller decrease.

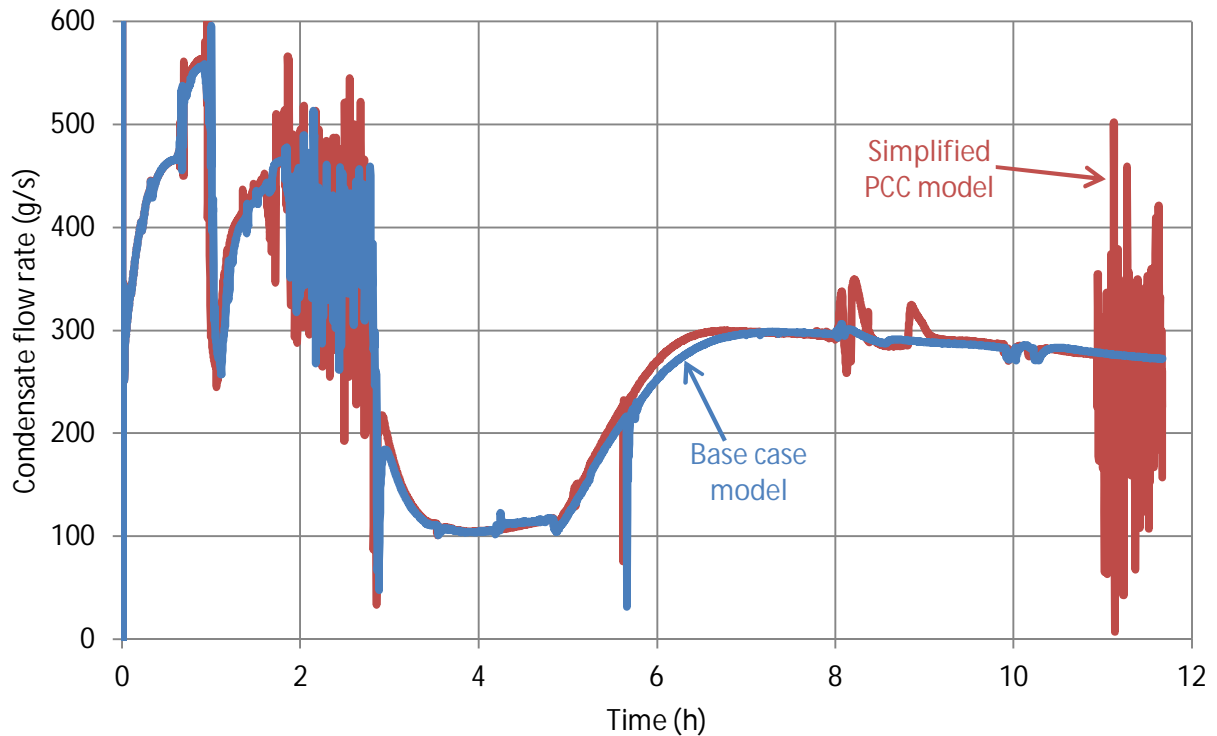


**Fig. 44.** Partial pressure of helium at the top of wetwell 2 (CV 56 in the MELCOR model, gas sampling port S2A.1 in the experiment).

#### 4.3.2 Simplified PCC Nodalization

In the base case model, the 20 PCC tubes were divided into 4 groups, each representing 5 tubes of equal length (Fig. 25). A simpler nodalization was also tried. Here all the 20 tubes were modeled as a single group. Division into three control volumes in the vertical direction was retained. This simplified nodalization is not able to calculate the flow reversal in some of the tubes due to the buoyancy caused by helium.

The condensation rate in the PCCs calculated with the base case model and the simplified model are compared in Fig. 45. The results are on the same level, but there is much more oscillation in the simplified model. The integral mass of steam that condensed during the whole experiment is 0.7 % larger with the simplified model than with the base case model.



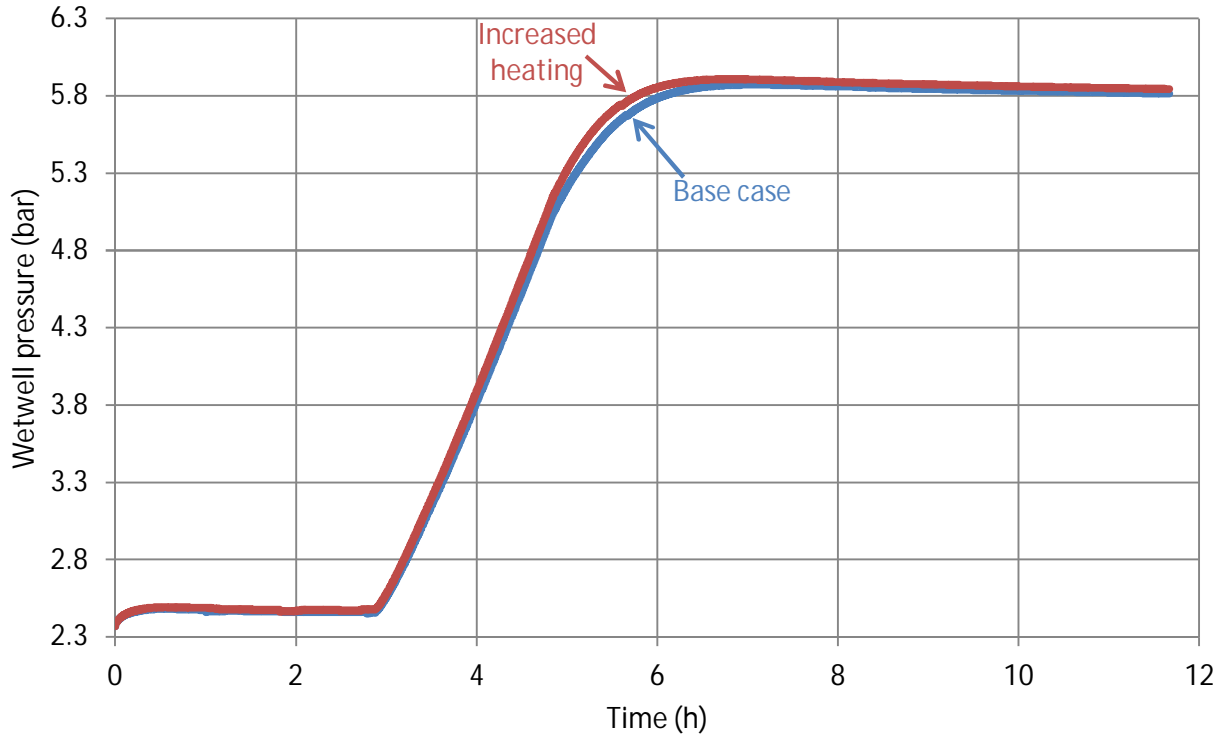
**Fig. 45.** PCC condensate flow rate, sum of three PCC units. Comparison between the base case model and the simplified PCC nodalization.

#### 4.3.3 Increased Heating Power

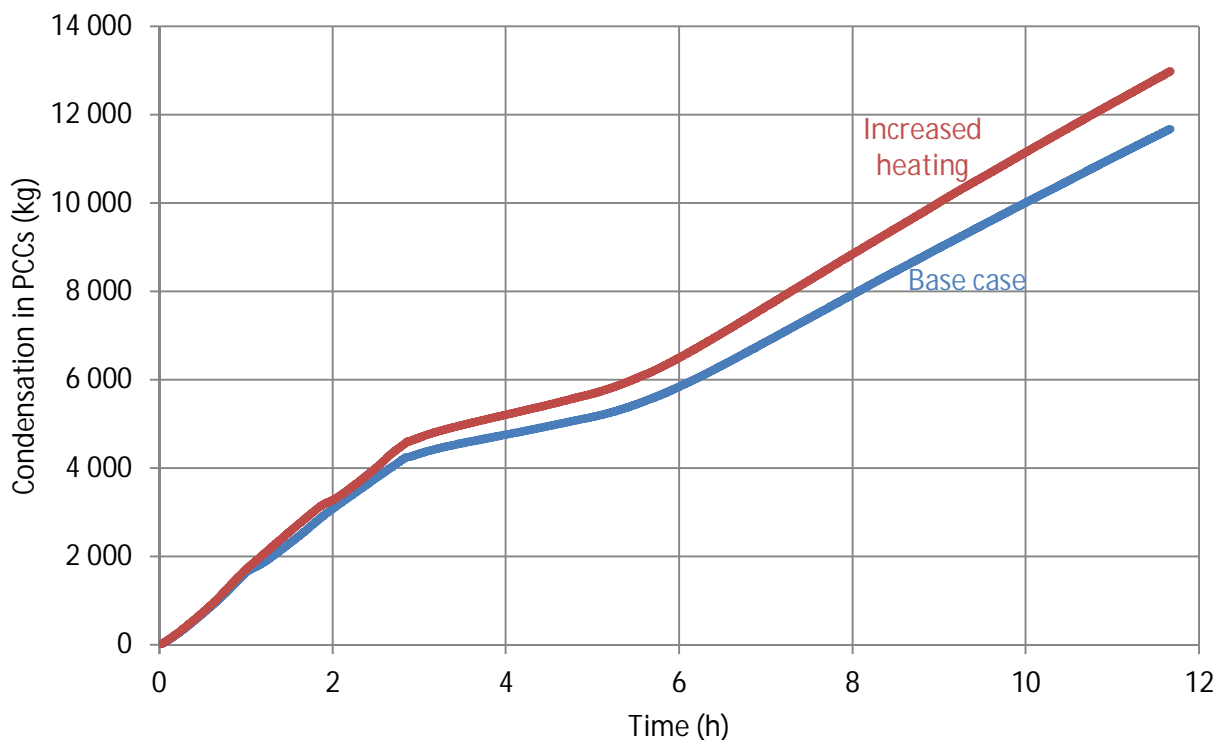
In order to get more insight into the operation of the PCCs, an imaginary case was calculated with 10 % higher heating power than what was used in the experiment. The wetwell pressure in both cases is plotted in Fig. 46. The increased heating power had a negligible effect on the pressure. Between 5 and 6 h there is a period when the increased heating power resulted in a small increase of pressure.

Fig. 47 shows a comparison of the integral mass of steam that condensed in the PCCs. The 10 % higher heating power resulted in 11.1 % more condensation. These results show that the PCCs have excess capacity. They would be able to handle at least 10 % higher power than what was used in the experiment, without causing any significant increase in pressure.





**Fig. 46.** Pressure in the wetwell. Comparison between the base case simulation and a case with 10 % higher heating power.



**Fig. 47.** Integral condensation, sum of three PCC units. Comparison between the base case simulation and a case with 10 % higher heating power.

## 5 Conclusions

A literature review of passive containment cooling system experiments was performed. Nine test facilities were found for thermal-hydraulic testing. The ESBWR condenser appears the

most extensively tested. Also the Kerena condenser has undergone lots of testing. Experiments of horizontal ABWR-type condensers were more difficult to find in publications.

Aerosol deposition in a condenser could weaken its efficiency due to flow blockage or fouling of heat exchange surfaces. Decay heat generated by the deposited aerosols could also have an effect on the condenser operation. On the other hand, the condensers could work as traps of radioactive aerosols and thereby reduce emissions to the environment. Scarce experimental data was found about aerosol deposition in condensers.

Lehtinen et al. (2002) experiments on condensation and aerosol deposition in a vertical tube were simulated with MELCOR 2.1. These tests extend the earlier MELCOR condensation validation calculations (Sevón 2010) to higher non-condensable gas concentrations. The calculated condensation rates were within 8 % of the measurements. The calculated aerosol deposition was within 10 percentage units of the measurements. Dividing the 85 cm long tube into three control volumes and heat structures was found sufficient.

The main topic of this report is modeling the PANDA T1.1 experiment with MELCOR 2.1. The PANDA facility represents the ESBWR containment at 1:40 scale. Three passive containment condensers (PCCs), each consisting of 20 vertical tubes, were connected to the facility. The T1.1 experiment simulated a main steam line break accident. Helium was released to the facility as a simulant of hydrogen. A detailed MELCOR model, consisting of 104 control volumes, was made.

A problem in calculating the PANDA test was an uncertainty in the amount of helium injected to the facility. According to the test report, 92 kg of helium was injected. However, from helium concentration measurements with a mass spectrometer, it can be calculated that the absolute maximum amount of helium in the facility was 81 kg. A best-estimate helium mass is 75 kg. The 6 kg difference between the maximum and best-estimate is caused by uncertainties in helium concentration in the GDCS tank because no helium concentration measurement was made there. If the experiment is simulated with MELCOR or GOTHIC (Paladino et al. 2003a) using the reported 92 kg of helium, the pressure and the helium concentrations are significantly overestimated. This further justifies the conclusion that the actual amount of injected helium was less than 92 kg. The best-estimate mass, 75 kg, was used in the MELCOR calculations.

The 20 tubes in a PCC unit were divided into 4 groups in the MELCOR model. Each group represented 5 tubes of equal length. Each of the 4 groups was divided into 3 control volumes of equal lengths in the vertical direction. Thus, the PCC tubes were modeled as 12 control volumes per one PCC unit. Such small control volumes required using short time steps, 0.02 s. A full-scale condenser used in a real containment is bigger. Thus, the control volumes would also be bigger, and longer time steps could probably be used.

It was found out that careful modeling of the condensate drainage is important for PCC calculations. When a smooth vertical structure is modeled as several heat structures, it is obvious that MELCOR's film tracking model is used to properly calculate the condensate film thickness in the lower structures. But a more difficult issue is the treatment of the condensate in places where the structure is not smooth and the water probably flows down as droplets. In MELCOR's default treatment, the condensed water would form a water pool at the bottom of the control volume. From there the water would flow down through all control volumes stacked vertically on top of each other. There would be a tiny levitating water pool in each of the volumes. This was found to cause serious oscillation in the calculation.

The problem of levitating pools was solved by setting a small auxiliary heat structure to the PCC drain line. MELCOR's film tracking model was used for guiding the drainage directly onto this auxiliary heat structure and from there to the drain line, instead of forming levitating

pools inside the PCC unit. Another possible solution to the oscillation caused by the levitating pools would be transferring the condensate to the Spray package. This was not tried because MELCOR Users' Guide recommends not to use multiple spray trains in one control volume.

The calculations overestimate the wetwell pressure by 0.07 bar and the drywell pressure by 0.11 bar at the end of the experiment. These are considered negligible deviations. A short-term dip of about 0.2 bar in the drywell pressure took place in the beginning of the calculation. This caused a short opening of the vacuum breaker valve, which did not occur in the experiment. This also caused some fluctuation in the operation of the PCCs. The helium concentrations are calculated with the accuracy that one can expect for a lumped parameter code. There was some helium stratification in the drywells, but the MELCOR model calculates well-mixed drywell atmospheres at all times.

Before helium injection, the amount of steam condensation in the PCCs is underestimated by 2 %. At the end of the experiment, the underestimation has increased to 7 %. A similar deviation between the measurement and calculation can be seen in the water levels of the PCC pools. Some significant deviations occur in the temperatures in some of the PCC tubes and in the PCC lower headers. These deviations may be caused by small differences in the non-condensable gas concentrations or differences in the direction of gas flow in the tubes.

12 out of 60 PCC tubes had thermocouples inside the tubes or in the tube walls. At the end of the experiment, 10 of these 12 tubes show higher temperatures at the bottom of the tube than at the top. This inverse temperature gradient might indicate that the flow direction in the tube is upwards. Such flow reversal could be caused by the buoyancy because helium is lighter than steam. In the MELCOR calculation, the flow in the longest group of tubes in all three PCC units reverses direction during the helium injection. The reversed flow continues until the end of the experiment.

A simplified PCC nodalization was also tested. All the 20 PCC tubes were modeled as a single group, while there were four groups in the base case model. The simplified model is not able to calculate the flow reversal in some of the tubes. The simplification caused only 0.7 % difference in the total mass of steam condensed in the PCCs. However, there was much more oscillation in the results of the simplified model.

In (Sevón 2010), it was found out that modifying condensate film Reynolds number limits from the MELCOR defaults to values commonly found in heat transfer textbooks improved the results significantly, when calculating Purdue University experiments on steam condensation in a tube. In the calculations of the Lehtinen et al. experiments and of the PANDA experiment, presented in this report, the difference between the default and modified Reynolds number limits was negligible. The reason is probably that in these experiments the condensate film flow was in the laminar regime with both default and modified parameters for most of the time.

In order to get more insight into the operation of the PCCs, an imaginary case with 10 % higher heating power in the RPV was calculated. Increasing the power had almost no effect on the pressure. The PCCs used in the experiment had so much excess capacity that they would be able to handle at least 10 % higher power than what was used in the experiment.

It is concluded that MELCOR was able to calculate the performance of the passive containment condensers in the PANDA experiment with an accuracy of about 7 %. In the absence of helium the accuracy was 2 %. These are sufficiently good values for using the model in simulating ESBWR accident scenarios. This conclusion naturally applies only for those conditions that were encountered in the experiment. In particular, the concentration of non-condensable gases is very significant for the performance of a condenser. The experiment was limited to less than 20 % non-condensable gas concentrations.

There were some significant deviations in the temperatures inside the condenser. If one is interested in detailed flow fields and local temperatures in a condenser, some more advanced thermal-hydraulic code should be used. Possible future work in this field could include testing more detailed nodalization in the vertical direction in the PCC tubes or in the PCC pool. Finding the capacity limits of the condenser by using even higher heating power or higher non-condensable gas concentration could also be interesting.

## References

- Ambrosini, W., Bucci, M., Forgone, N., Manfredini, A. & Oriolo, F. 2009.** *Experiments and modelling techniques for heat and mass transfer in light water reactors*. Science and Technology of Nuclear Installations, vol. 2009, article id 738480.  
<http://downloads.hindawi.com/journals/stni/2009/738480.pdf>
- Arai, K., Kurita, T., Nakamaru, M., Fujiki, Y., Nakamura, H., Kondo, M., Obata, H., Shimada, R. & Yamaguchi, K. 2002.** *Multi-dimensional thermal-hydraulic analysis for horizontal tube type PCCS*. International Conference on Nuclear Engineering (ICONE 10), Arlington, Virginia, 14–18 April 2002. Paper 22442.
- Arai, K., Murase, A., Hamazaki, R. & Kuroki, M. 2008.** *AB1600 – Progress of ABWR technology toward next generation ABWR*. Nuclear Engineering and Design, vol. 238, p. 1902–1908.
- Auban, O., Paladino, D., Candreia, P., Huggenberger, M. & Strassberger, H.J. 2003.** *Overview of some new PANDA tests results: Effects of light gases on passive safety systems*. International Congress on Advances in Nuclear Power Plants (ICAPP '03), Cordoba, Spain, 3–7 May 2003.
- Beard, J.A. 2006.** *ESBWR Overview*. GE Energy.  
<http://www.ne.doe.gov/np2010/pdfs/esbwrOverview.pdf>
- Dreier, J., Aubert, C., Huggenberger, M., Strassberger, H.J., Meseth, J. & Yadigaroglu, G. 1999.** *The PANDA tests for the SWR 1000 passive containment cooling system*. International Conference on Nuclear Engineering (ICONE 7), Tokyo, Japan, 19–23 April 1999. Paper 7316.
- Faluomi, V. & Aksan, S.N. 1998.** *RELAP5 capabilities in thermal-hydraulic prediction of SBWR containment behaviour: PANDA steady state and transient tests evaluation*. In: Experimental Tests and Qualification of Analytical Methods to Address Thermohydraulic Phenomena in Advanced Water Cooled Reactors. IAEA, 2000, p. 315–326. (IAEA-TECDOC-1149.) [http://www-pub.iaea.org/MTCD/publications/PDF/te\\_1149\\_prn.pdf](http://www-pub.iaea.org/MTCD/publications/PDF/te_1149_prn.pdf)
- Fethke, M., Jaegers, H. & Hicken, E.F. 1998.** *First experiments of the passive safety system building condenser in the NOKO test facility and post-test calculations using the RALOC code*. International Conference on Nuclear Engineering (ICONE 6), San Diego, California, 10–14 May 1998. Paper 6506.
- Friesen, E., Meseth, J., Guentay, S., Suckow, D., López Jiménez, J., Herranz, L., Peyres, V., De Santi, G.F., Krasenbrink, A., Valisi, M. & Mazzocchi, L. 2001.** *Containment behaviour in the event of core melt with gaseous and aerosol releases (CONGA)*. Nuclear Engineering and Design, vol. 209, p. 253–262.
- Gröhn, A., Suonmaa, V., Auvinen, A., Lehtinen, K.E.J. & Jokiniemi, J. 2009.** *Reduction of fine particle emissions from wood combustion with optimized condensing heat exchangers*. Environmental Science & Technology, vol. 43, p. 6269–6274.

- Hart, J., Slegers, W.J.M., de Boer, S.L., Huggenberger, M., Lopez Jimenez, J., Munoz-Cobo Gonzalez, J.L. & Reventos Puigjaner, F. 2001.** *TEPSS – Technology enhancement for passive safety systems*. Nuclear Engineering and Design, vol. 209, p. 243–252.
- Hicken, E.F., Jaegers, H., Schaffrath, A. & Weiss, F.-P. 2000.** *The NOKO/TOPFLOW facility for natural convection flow*. In: Natural Circulation Data and Methods for Advanced Water Cooled Nuclear Power Plant Designs. IAEA, 2002, p. 213–226. (IAEA-TECDOC-1281.) [http://www-pub.iaea.org/MTCD/publications/PDF/te\\_1281\\_prn.pdf](http://www-pub.iaea.org/MTCD/publications/PDF/te_1281_prn.pdf)
- Huggenberger, M., Auban, O., Paladino, D., Candreia, P. & Strassberger, H.J. 2002.** *Description of PANDA Facility Including Test Specification*. Paul Scherrer Institut. (TM-42-02-16, ALPHA-02-07-0, EVOL-TEMPEST-D06A.)
- Incropera, F.P. & DeWitt, D.P. 2002.** *Fundamentals of Heat and Mass Transfer*. Fifth edition. John Wiley & Sons.
- Ishii, M., Yoo, Y.-J., Cheng, L., Choi, S.W., Yang, J., Aksan, N., Kondo, M., Nakamura, H. & Yonomoto, T. 2007.** *Behavior of Containment Emergency Systems*. [http://www.iaea.org/NuclearPower/Downloads/NaturalCirculation/SOAR/SOAR\\_Phenomena\\_4\\_Final.pdf](http://www.iaea.org/NuclearPower/Downloads/NaturalCirculation/SOAR/SOAR_Phenomena_4_Final.pdf)
- Kataoka, K., Arai, K. & Yokobori, S. 1998.** *TRAC analyses and GIRAFFE tests for PCCS performance prediction*. In: Experimental Tests and Qualification of Analytical Methods to Address Thermohydraulic Phenomena in Advanced Water Cooled Reactors. IAEA, 2000, p. 401–417. (IAEA-TECDOC-1149.) [http://www-pub.iaea.org/MTCD/publications/PDF/te\\_1149\\_prn.pdf](http://www-pub.iaea.org/MTCD/publications/PDF/te_1149_prn.pdf)
- Kojima, Y., Arai, K., Kurita, T., Oikawa, H., Akinaga, M., Tobimatsu, T., Yanagisawa, H., Tahara, M. & Hamazaki, R. 2010.** *Performance of horizontal U-tube type passive containment cooling system in a BWR*. International Congress on Advances in Nuclear Power Plants (ICAPP '10), San Diego, California, 13–17 June 2010. Paper 10273.
- Kondo, M., Nakamura, H., Anoda, Y., Saishu, S., Obata, H., Shimada, R. & Kawamura, S. 2002.** *Roll wave effects on annular condensing heat transfer in horizontal PCCS condenser tube*. International Conference on Nuclear Engineering (ICONE 10), Arlington, Virginia, 14–18 April 2002. Paper 22403.
- Lehtinen, K.E.J., Hokkinen, J., Auvinen, A., Jokiniemi, J.K. & Gamble, R.E. 2002.** *Studies on steam condensation and particle diffusiophoresis in a heat exchanger tube*. Nuclear Engineering and Design, vol. 213, p. 67–77.
- Leyer, S., Wich, M. & Schäfer, H. 2008.** *SWR 1000 integral and full scale tests of the passive safety systems*. International Congress on Advances in Nuclear Power Plants (ICAPP '08), Anaheim, California, 8–12 June 2008. Paper 8054.
- Leyer, S., Maisberger, F., Herbst, V., Doll, M., Wich, M. & Wagner, T. 2010.** *Status of the full scale component testing of the KERENA™ emergency condenser and containment cooling condenser*. International Congress on Advances in Nuclear Power Plants (ICAPP '10), San Diego, California, 13–17 June 2010. Paper 10257.
- Liao, Y., Vierow, K. & Han, J.T. 2008.** *MELCOR validation against a PUMA facility main steam line break integral test*. International Congress on Advances in Nuclear Power Plants (ICAPP '08), Anaheim, California, 8–12 June 2008. Paper 8189.
- Lübbesmeyer, D., Aksan, S.N., Aubert, C., Dreier, J., Huggenberger, M. & Fischer, O. 1999.** *ISP-42 Description of the PANDA-Facility*. Paul Scherrer Institut. (TM-42-98-41, ALPHA-836-1, Rev. 1.)

- Lübbesmeyer, D. & Aksan, S.N. 2003.** *ISP42 (PANDA tests) open phase comparison report.* OECD Nuclear Energy Agency. (NEA/CSNI/R(2003)7.)  
<http://www.oecd-nea.org/nsd/docs/2003/isp-42/Open.pdf>
- Maheshwari, N.K., Saha, D., Chandraker, D.K., Venkat Raj, V. & Kakodkar, A. 2001.** *Studies on the behaviour of a passive containment cooling system for the Indian Advanced Heavy Water Reactor.* Kerntechnik, vol. 66, p. 15–20.
- Muñoz-Cobo, J.L., Peña, J., Herranz, L.E. & Pérez-Navarro, A. 2005.** *Steam condensation on finned tubes, in the presence of non-condensable gases and aerosols: Influence of impaction, diffusiophoresis and settling on aerosol deposition.* Nuclear Engineering and Design, vol. 235, p. 1225–1237.
- Oh, S. 2004.** *Experimental and Analytical Study of the Effects of Noncondensable Gas in a Passive Condenser System.* Ph.D. thesis. Purdue University.
- Paladino, D., Auban, O., Huggenberger, M. & Andreani, M. 2003a.** *Investigation of light gas effects on passive containment cooling system in ALWR.* International Topical Meeting on Nuclear Reactor Thermal Hydraulics (NURETH-10), Seoul, Korea, 5–9 October 2003. Paper F00206.
- Paladino, D., Auban, O., Huggenberger, M., Candraia, P. & Strassberger, H.J. 2003b.** *PANDA System Test T1.1 Base Case with Helium.* Paul Scherrer Institut. (TM-42-02-22, ALPHA-02-09-0, EVOL-TEMPEST-D06B.)
- Paladino, D., Auban, O., Huggenberger, M. & Dreier, J. 2011.** *A PANDA integral test on the effect of light gas on a passive containment cooling system (PCCS).* Nuclear Engineering and Design, vol. 241, p. 4551–4561.
- Parlatan, Y., Boyer, B.D., Jo, J. & Rohatgi, S. 1996.** *Analysis of PANTHERS full-scale heat transfer tests with RELAP5.* ASME/JSME International Conference on Nuclear Engineering (ICONE 4), New Orleans, Louisiana, 10–14 March 1996.  
[http://www.osti.gov/energycitations/product.biblio.jsp?osti\\_id=197819](http://www.osti.gov/energycitations/product.biblio.jsp?osti_id=197819)
- Sandia National Laboratories. 2011.** *MELCOR Computer Code Manuals. Vol. 2: Reference Manual. Version 2.1 September 2011.* Thermal Hydraulic (CVH and FL) Packages Reference Manual. (NUREG/CR-6119, Vol. 2, Rev. 3194.) Draft.
- Sevón, T. 2010.** *MELCOR Simulations of Steam Condensation in a Condenser Tube.* VTT Technical Research Centre of Finland. (Research report VTT-R-01503-10.)  
<http://www.vtt.fi/inf/julkaisut/muut/2010/VTT-R-01503-10.pdf>
- Sinha, R.K. & Kakodkar, A. 2006.** *Design and development of the AHWR – the Indian thorium fuelled innovative nuclear reactor.* Nuclear Engineering and Design, vol. 236, p. 683–700.
- Stempniewicz, M.M. 2000.** *Analysis of PANDA passive containment cooling steady-state tests with the SPECTRA code.* Nuclear Technology, vol. 131, p. 82–101.
- Stosic, Z.V., Brettschuh, W. & Stoll, U. 2008.** *Boiling water reactor with innovative safety concept: The generation III+ SWR-1000.* Nuclear Engineering and Design, vol. 238, p. 1863–1901.
- STUK. 2009.** *Preliminary Safety Assessment of Loviisa 3 Nuclear Power Plant Project. Appendix 1: Feasibility Assessment of Plant Alternatives.* Radiation and Nuclear Safety Authority.  
[http://www.stuk.fi/ydinturvallisuus/ydinvoimalaitokset/uudet\\_laitosyksikot/en\\_GB/uudet\\_laitosyksikot/\\_files/83141798951583905/default/STUK\\_Fortum\\_PreliminarySafetyAssessment\\_plant\\_alternatives\\_appendix1.pdf](http://www.stuk.fi/ydinturvallisuus/ydinvoimalaitokset/uudet_laitosyksikot/en_GB/uudet_laitosyksikot/_files/83141798951583905/default/STUK_Fortum_PreliminarySafetyAssessment_plant_alternatives_appendix1.pdf)

**Suonmaa, V. 2006.** *Reducing the Fine Particle Emissions from Wood Combustion Using Condensing Heat Exchangers.* Master of Science thesis. University of Kuopio. (In Finnish.)

**Tuomainen, M. 2003.** *Fluent Simulation of PCC Behaviour in PANDA Test T1.2.* VTT Technical Research Centre of Finland. (Research report PRO1/P7016/03, EVOL-TEMPEST-D09b.)

**Zhou, W., Henderson, G. & Revankar, S.T. 2010.** *Condensation in a vertical tube bundle passive condenser – Part 1: Through flow condensation.* International Journal of Heat and Mass Transfer, vol. 53, p. 1146–1155.